Bull Earthquake Eng (2018) 16:5453–5488
https://doi.org/10.1007/s10518-018-0384-y

ORIGINAL RESEARCH PAPER

A statistical assessment on global drift ratio demands of mid-rise RC buildings using code-compatible real ground motion records

Mehmet Palanci[1] · **Ali Haydar Kayhan**[2] · **Ahmet Demir**[2]

Received: 4 August 2017 / Accepted: 1 May 2018 / Published online: 21 May 2018

Abstract Over the past 20 years, significant socio-economic losses have been encountered in Turkey due to several moderate to large earthquakes. The studies published after the earthquakes concurringly emphasized that multistory reinforced concrete (RC) buildings, mostly 3–7 story ones, collapsed or were heavily damaged as a result of inadequate seismic performance. Global drift ratio demands are mostly used as a representative quantity for determining the behavior of structures when subjected to earthquakes. In this study, three representative mid-rise RC buildings are analyzed by nonlinear time history analysis using code-compatible real ground motion record sets and the calculated global drift ratio demands of these buildings are statistically evaluated. Ground motion record sets compatible with the design spectrum defined for local soil classes in the Turkish Earthquake Code (TEC-2007) are used for the analyses. In order to evaluate the effect of the number of ground motions on drift ratio demands, five different ground motion record sets with 7, 11 and 15 ground motion records are used separately for each local soil class. Results of this study indicate that (1) the dispersion of global drift ratio demands calculated for individual ground motion records in record sets is high, (2) local soil class has no significant effect on dispersion. However, dispersion increases in a direct proportion to the number of ground motion records in a record set, (3) the mean of global drift ratio demands calculated for different ground motion record sets may differ although they are compatible with the same design spectrum, (4) the mean of the drift demands obtained from different ground motion record sets compatible with a particular design spectrum can be accepted as simply random samples of the same population at 95% confidence level.

✉ Mehmet Palanci
mehmetpalanci@arel.edu.tr

Ali Haydar Kayhan
hkayhan@pau.edu.tr

Ahmet Demir
ademir@pau.edu.tr

[1] Department of Civil Engineering, Istanbul Arel University, Istanbul, Turkey

[2] Department of Civil Engineering, Pamukkale University, Denizli, Turkey

Keywords RC buildings · Nonlinear dynamic analysis · Statistical evaluation

1 Introduction

One of the largest potential sources of casualties and damage for inhabited areas due to natural hazard is earthquakes. Every year, many earthquakes varying in size and destructive potential occur worldwide. Earthquakes, especially moderate and large ones can cause serious socio-economic losses. The amount of socio-economic losses that result from an earthquake depends on the size, depth and location of the earthquake, the intensity of the ground shaking and related effects on the building inventory, and the vulnerability of that building inventory to damage.

Turkey is a country under the threat of damaging earthquakes and over the past 20 years significant socio-economic losses have occurred resulting from several moderate and large earthquakes, such as 1998 Adana–Ceyhan ($M_s = 6.3$), 1999 Kocaeli ($M_w = 7.4$), 1999 Düzce ($M_w = 7.2$), 2002 Afyon–Sultandagi ($M_w = 6.3$), 2003 Bingöl ($M_w = 6.4$) and 2011 Van ($M_w = 7.2$). The studies published after these earthquakes regarded the seismic performance of the buildings, the observed structural damages and the reasons for these damages (Sezen et al. 2000; Adalier and Aydingun 2001; Akkar et al. 2005a; Celep et al. 2011; Taskin et al. 2013; Yon et al. 2013; Korkmaz 2015). These studies concurringly emphasized that multistory RC buildings, especially 3–7 story ones collapsed or were heavily damaged due to inadequate seismic performance. The main reasons for the observed damages can be classified as poor concrete quality, insufficient reinforcement detailing, soft and weak story mechanisms, short column problems, insufficient shear walls, large and heavy overhangs, strong beams-weak columns and poor construction practices (Inel et al. 2008; Arslan 2010; Ilki and Celep 2012). The observed insufficient seismic performance and structural properties of the existing RC buildings after major earthquakes showed that there is a critical discrepancy between the presence of seismic code regulations and the existing situation. This outcome is mainly based on the lack of influential control mechanisms for the design and construction practices (Ilki and Celep 2012). The experiences gained from the evaluation of the studies may be very useful for predicting the expected behavior of existing buildings in future earthquakes and taking the necessary measures to reduce possible damages and losses.

Recently, performance based design methods have been used extensively for the seismic design or evaluation of buildings. Design criteria are expressed in terms of achieving stated performance objectives when the structure is subjected to stated levels of seismic hazard. Thus, performance objectives, determination of seismic demands and performance evaluation are three principal steps of the performance based design. The SEAOC Vision 2000 document (SEAOC Vision 2000 Committee 1995), one of the first major documents on performance based design, listed various advanced performance based design or evaluation approaches such as (a) displacement-based design, (b) energy-based design and (c) comprehensive design considering lifecycle cost. So far, the displacement based design approach has been widely adopted and structures are being designed in accordance with target response parameters such as maximum displacement, ductility demand, global and inter-story drift ratio etc. (Priestley et al. 2007). The same parameters are also used to define various performance levels or limit states (ATC-40 1996; FEMA-440 2005).

Among the target response parameters, global and inter-story drift ratio demands can be accepted as the most commonly used ones. One of the most important steps in performance

based design and/or the evaluation of structures is the determination of demands for seismic loads related to considered seismic level and this requires accurate structural modeling and analysis. A nonlinear time history analysis of a three-dimensional structural model is the most comprehensive and accurate analytical method to evaluate the seismic demands. Nowadays, this analysis method has been increasingly preferred because of the developments in the processing power of computers and the software industry. However, a nonlinear time history analysis of three-dimensional structures is complex. For this reason, the simpler two-dimensional frames (Akkar et al. 2005b; Medina and Krawinkler 2005; García and Miranda 2006; Hatzigeorgiou and Liolios 2010; García and Miranda 2010; Ghaffarzadeh et al. 2013) or single degree of freedom (SDOF) systems (Bazzurro and Luco 2005; D'Ambrisi and Mezzi 2005; García and Miranda 2007; Lin and Miranda 2009; Hatzigeorgiou and Beskos 2009; Hou and Qu 2015) are also preferred as structural analysis models. In these studies, different criteria are used in the selection of ground motion records for nonlinear time history analyses.

It should be noted that ground motion records affect the seismic demands used for seismic design and/or performance evaluation (Katsanos et al. 2010; Araújo et al. 2016). Therefore, it is important to use suitable ground motion records for time history analyses, based on the seismicity and local soil conditions of a structure to make a reliable estimation of the seismic demands (Iervolino et al. 2010a; Han et al. 2014). In order to perform a time history analysis, relatively similar procedures with minor different requirements are described in modern seismic codes (TEC-2007 2007; FEMA-368 2001; EUROCODE-8 2004; ASCE 07-05 2006; GB 2010). For example, synthetic, artificial, or real ground motion records could be used as long as they are compatible with regional design spectra defined in the seismic codes within a stated period range. Usually, according to these codes at least three ground motion records are required. The average of the structural responses can be used for seismic design and/or performance evaluation if at least seven ground motion records are selected, otherwise the maximum of structural responses should be considered.

In modern seismic design codes, the ground motion selection process only considers the average spectrum of the selected ground motions for time history analysis and the target design spectrum without considering random variability of the ground motion records. In addition, recent studies showed that it is possible to obtain different code-compatible ground motion record sets by selecting and scaling from hundreds of ground motion records available in digital databases (Iervolino et al. 2008; Kayhan et al. 2011; Kayhan 2016). Hence, estimated seismic demands representing the structural responses to seismic excitation vary significantly and could be accepted as random variables that change according to code-compatible record sets used for nonlinear time history analyses (Cantagallo et al. 2014; Macedo and Castro 2017). Recently, various studies were carried out to investigate the efficiency of the selecting and scaling of ground motion records according to various seismic codes. Reyes and Kalkan (2012) used theoretical models with varying lateral strength reduction factors (R) and natural vibration periods to evaluate the accuracy of the ground motion scaling procedure of ASCE 07-10 (2010) in terms of structural responses and as a result they observed high variations. Katsanos and Sextos (2013) developed an integrated software environment to select structure specific ground motions according to the European and US seismic codes and applied it to irregular RC buildings. Results of this study have demonstrated the very high variability in both structural and member responses. Sextos et al. (2011) used the EUROCODE-8 based earthquake record selection procedure for the evaluation, considering the irregular damaged RC buildings and highlighted the large dispersion and demonstrated the limitations of the EUROCODE-8 earthquake ground

motion selection framework for the assessment of both elastic and inelastic structural response of multi-story irregular RC buildings. Kayhan and Demir (2016) used two dimensional generic RC frames to evaluate the code-compatible procedure of the TEC-2007 in different soil conditions using roof and inter-story drift ratios by various record sets that have seven ground motions. According to Kayhan and Demir, the variation of seismic demands and inter-story drift ratios are significantly high. Shome et al. (1998) pointed out that the number of records required to obtain an estimate of the median response to within a defined confidence interval depends on the standard deviation of the response. Therefore, the number of records to be used should depend on both the procedure used to select and scale the accelerograms and the nature of the structural response being investigated. Hancock et al. (2008) stated that the number of required records and the degree of bias both systematically decrease as one applies more constraint on the scaling and matching of accelerograms. Hence, the number of records that are required to obtain a robust estimate of the inelastic response may be significantly reduced through the use of the spectrally matched, wavelet-adjusted, accelerograms. Hancock et al. also stated that the degree of bias may be accounted for through the use of factors as commonly adopted elsewhere in seismic design codes.

The aim of this study is to investigate the effect of the code-based record selection methods on the global drift ratio demands of RC buildings in terms of mean and variation calculated by nonlinear time history analyses using different code-compatible sets of ground motion records. The effect of local soil conditions and the number of ground motions in the record sets used for the nonlinear time history analyses on drift ratio demands is also investigated. In accordance with these aims, three mid-rise RC buildings that represent a major portion of the existing RC building stock in Turkey are considered. Five ground motion record sets with 7, 11 and 15 ground motion records are used separately for the nonlinear time history analysis of the buildings considering various local soil classes defined in the TEC-2007. The lateral strength and displacement capacity of the buildings are determined by pushover analyses and the dynamic characteristics of the buildings are represented by equivalent SDOF systems. The maximum drift ratio demands using individual ground motion records in the record sets and the mean and the coefficient of variation of the demands are calculated. A one way analysis of variance (ANOVA) is performed to evaluate the differences between the mean drift ratios demands calculated for different record sets compatible with the same design spectrum. Finally, the sampling distributions of the mean drift ratio demands are estimated for the buildings considering different local soil classes. Using the results of this study, various recommendations are suggested and also practical implications in the selecting and scaling of seismic codes in the assessment and design of structures are also discussed for practitioners in civil engineering.

2 The representative RC buildings

In the present study, existing mid-rise buildings in Turkey are represented by a selection of three 5-story RC buildings, namely 5A, 5B and 5C. These buildings are typical RC frame buildings consisting of columns and beams without structural walls. The selected mid-rise RC buildings were designed in accordance with TEC-1975 and represent the general characteristics of existing RC buildings in Turkey. The nonlinear behavior of the selected buildings are determined by using 3-D nonlinear structural models and the required structural properties (cross-sectional dimensions of members, reinforcement details, filled walls,

dead and moving loads on slabs, etc.) are obtained from their own architectural and RC design projects.

The floor plans for buildings 5A and 5C are given in Fig. 1 and the floor plan for building 5B is given in Fig. 2. For building 5A, the height of the base story is 3.40 m, the first story is 3.00 m and the rest of the stories are 2.80 m. The cross-sectional dimension of the beams in all story plans is 0.20×0.50 m except K05 (0.20×0.60 m). The cross-sectional dimensions of the columns at the base story are given in Fig. 1. The longitudinal reinforcement ratio of the columns varies between 0.8 and 1.1%. The cross-sectional dimensions of some of the columns are reduced on the upper floors. It can be seen from Fig. 1 that all the columns are placed in the direction of the strong inertia (along y direction). This situation is also observed in significant parts of the existing structures in Turkey and it can be considered as a design mistake. Furthermore, three continuous moment-resisting frames can be seen along y direction but most of the frames along x direction are discontinuous. Continuous moment-resisting frames are the main part of the seismic force-resisting systems in buildings. As understood, building 5A has serious shortcomings in the x direction compared to the y direction in terms of both the placement of structural members and the continuous moment-resisting frames.

For building 5B, the height of the base story is 3.50 m and the other floors are 2.80 m. The cross-sectional dimensions of the beams on all floors are 0.25×0.60 m. The

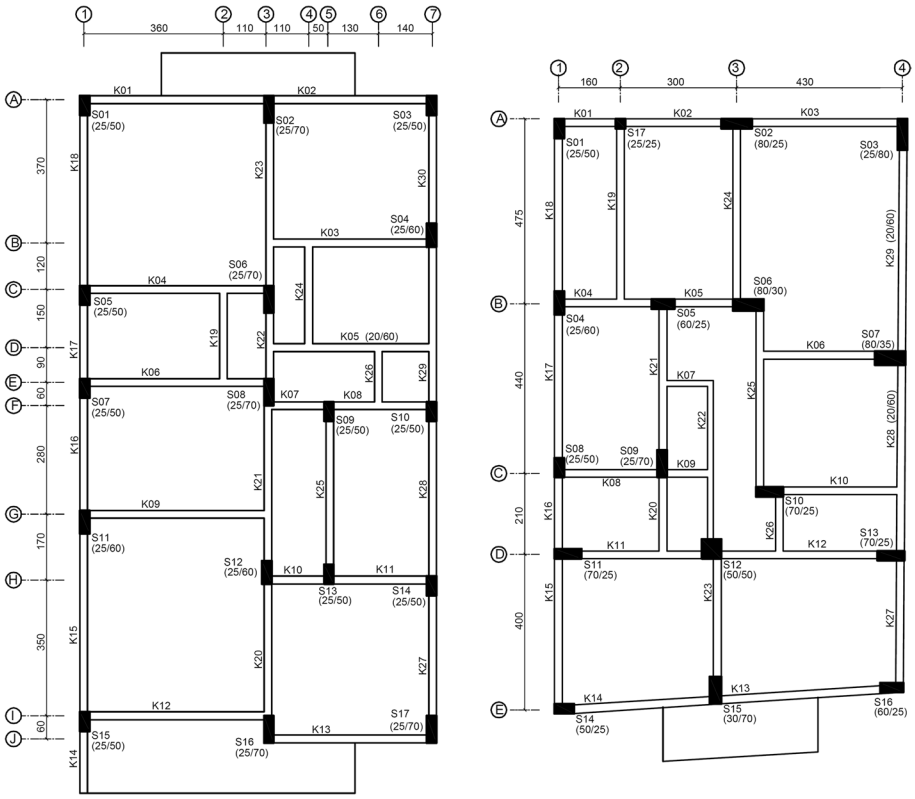

Fig. 1 Floor plan for buildings 5A and 5C (units in cm)

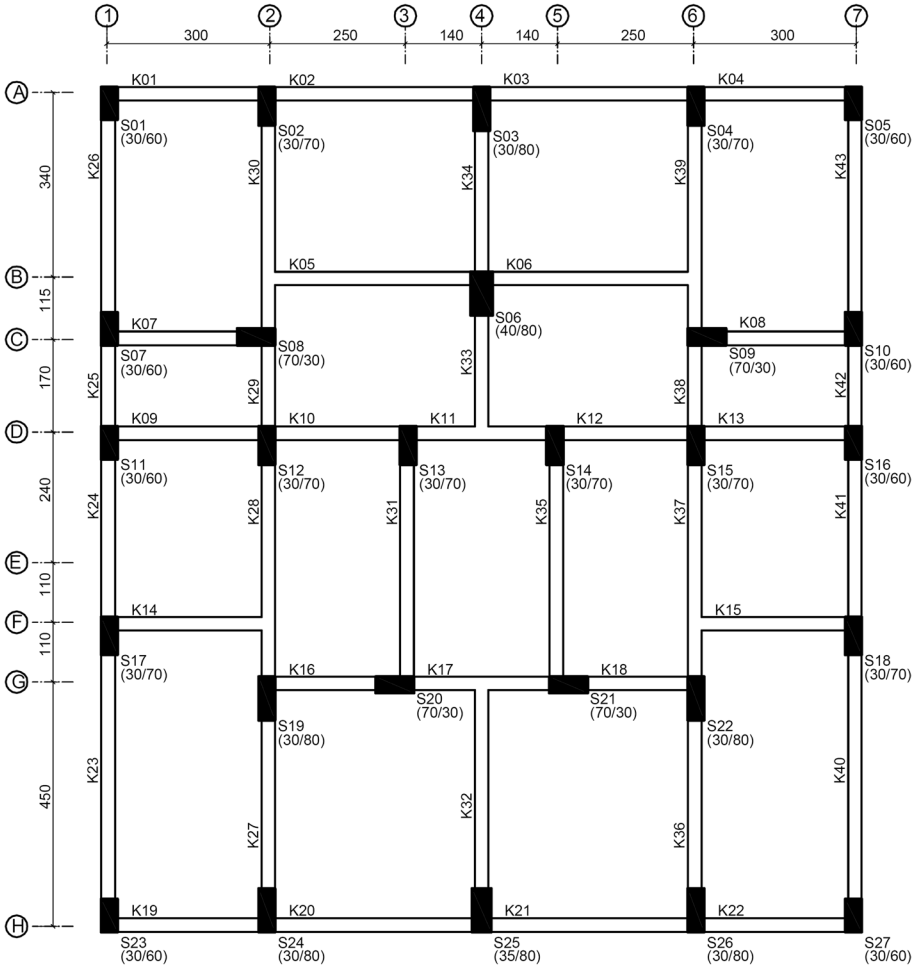

Fig. 2 Floor plan of building 5B (units in cm)

cross-sectional dimensions of the columns at the base story are given in Fig. 2. The longitudinal reinforcement ratio of the columns is around 1.0–1.1%. The cross-sectional dimensions of the beams and columns are the same for the upper floors.

The height of all the stories in building 5C is 2.80 m. The cross-sectional dimensions of the beams are 0.20×0.50 m except for K28 and K29 which are 0.20×0.60 m. The cross-sectional dimensions of the beams on the upper stories are the same as the base story. The longitudinal reinforcement ratio of the columns ranges between 1.0 and 1.5%. The cross-sectional dimensions of the columns are reduced on the upper floors as in building 5A. It can be seen from Fig. 1 that apart from the outer axis there is only one continuous moment-rising frame which is the axis D.

Most of the buildings constructed in accordance with the TEC-1975 are designed using C16 class concrete ($f_c = 16$ MPa) and S220 class reinforcement steel ($f_y = 220$ MPa). It is also observed that C16 and S220 class materials were used in the design projects of the selected representative buildings. For this reason, C16 and S220 materials are taken into

consideration for the structural model of the selected representative buildings. In the TEC-1975 and the more recent seismic design codes, various regulations such as the detailing transverse reinforcement of structural members, confinement regions at the end of structural members and beam-column connections are considered. However, it is a well-known fact that before the TEC-1997 there was non-compliance with these requirements in construction (Arslan 2010; Bal et al. 2008). For instance, at the ends of columns and beams, the stirrup spacing is expected to be equal to or smaller than 100 mm. Thus, in order to represent the insufficient transverse reinforcement of structural members, stirrup spacing is determined as 200 mm in the analysis of the representative buildings. The diameter of the stirrup for columns and beams is 8 mm. In the analysis models, dead and live loads, and the self-weight of beams, walls and slabs are taken into consideration.

2.1 Modeling approach

In this part of the study, information about the 3-D nonlinear analysis models of the representative buildings is given. The geometrical properties of each building, the cross-sectional dimensions and the reinforcement details of members and structural loads are directly obtained from the architectural and design projects of the buildings. The Sap2000 (CSI) structural analysis program has been used to prepare a fixed-based structural model and a pushover analysis of the buildings. The seismic weight of the stories is calculated by summing up the dead loads and 30% of the live loads according to the TEC-2007.

Structural members such as columns and beams are defined as nonlinear member frames. The nonlinear behavior of the structural members is represented by user-defined "lumped" plastic hinges and they are assigned to both ends of the columns and beams. Default or user-defined plastic hinges can be defined with the Sap2000 program. In Fig. 3, a typical force–deformation relationship of a plastic hinge is shown. It can be seen that points A, B, C, D and E can be used to express the behavior of the plastic hinge. Yield displacement is referred to by point B and point C refers to the maximum displacement capacity of members. Slight damage (SD), moderate damage (MD) and extensive damage (ED) regions can be determined after the calculation of IO, LS and CP deformation limits associated with the damage levels for the critical section of the ductile structural members. The coordinates of points A, B, C, D, and E and the deformation limits (IO, LS, CP) can be calculated using the cross-sectional properties, material qualities, longitudinal and transverse reinforcement details and axial load levels of structural members.

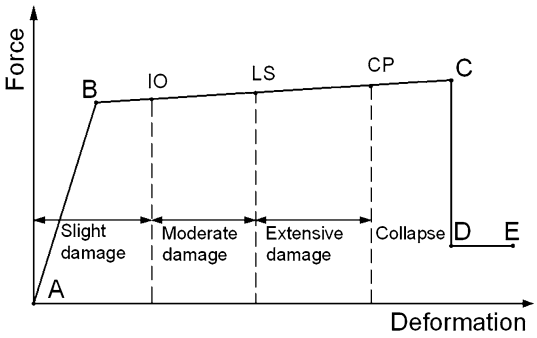

Fig. 3 Typical force–deformation relationship and deformation limits for damage levels

Moment–curvature analyses were performed for each structural member by spreadsheet software provided by Ersoy and Ozcebe (2001) and the properties of user-defined plastic hinges were determined. In the moment–curvature analysis, confined and unconfined concrete behaviors are represented by the Modified Kent-Park model (Scott et al. 1982) and typical stress–strain curve with strain hardening is used for reinforcing steel behavior (Mander 1984).

In Fig. 3, point the B indicates the elastic force and displacement capacity of members and can be calculated by the Sap2000 program using the effective stiffness of members. In the study, the points C and D are taken equal to the CP deformation limit as the CP limit defines the limit of the behavior before collapsing according to TEC-2007 and 20% of flexural strength of the member was assigned as the point D in y axis shown in Fig. 3. Furthermore, the point E is assumed as 2 times of the point D in deformation (x axis). The effective stiffness of beams is considered as *0.4EI* in the TEC-2007, and Eqs. (1a) and (1b) are recommended to calculate the effective stiffness of the columns depending on the axial load ratio. In Eqs. (1a) and (1b), N is axial load of column, A_c is column cross-sectional area and f_c is the compressive strength of concrete. Linear interpolation is recommended for axial load ratio between 10 and 40%.

$$0.4EI \quad if\ N/\left(A_c f_c\right) \le 0.10 \tag{1a}$$

$$0.8EI \quad if\ N/\left(A_c f_c\right) \ge 0.40 \tag{1b}$$

During the moment–curvature analysis, the damage limits of each member were also determined. The cross-sectional damage limits in the TEC-2007 at the critical sections of the structural members are given in Table 1 for the maximum concrete and steel strain limits. In Table 1, ρ_s and ρ_{sm} refer to the existing and required volumetric transverse reinforcement ratios given in the TEC-2007.

The moment–curvature relationship at the critical sections of members is converted to a moment-rotation relationship. During the conversion of the moment-rotation relationship, the plastic hinge length was taken as half of the cross-section height in the considered direction as given in the TEC-2007.

Recent studies have indicated that due to low concrete strength and insufficient transverse reinforcement, shear effects should also be considered in addition to flexural responses to represent the actual behavior of the structures (Palanci et al. 2014, 2016). For this reason, brittle shear effects are also considered and shear hinges are introduced for the critical regions of the beams and columns. Ductility is not considered for the shear hinges because of brittle failure of concrete in shear. Thus, if the shear force in the member reaches its shear strength, the member fails immediately. The shear strength of a member (V_r) is calculated by Eq. (2) as suggested in Turkish standards TS-500 (2000). In the equation, b_w and d represent width and the effective height of the cross-section, A_{sw} and f_y represent the cross-sectional area and the yield strength of shear reinforcement, s represents

Table 1 Cross-sectional damage limits in the TEC-2007

Sectional damage	Concrete strain (ε_c)	Steel strain (ε_s)
Slight damage	0.0035	0.010
Moderate damage (MD)	$0.0035+0.010(\rho_s/\rho_{sm}) \le 0.0135$	0.040
Extensive damage (ED)	$0.0040+0.014(\rho_s/\rho_{sm}) \le 0.0180$	0.060

the distance between the transverse reinforcements and N/A_c is the ratio of axial load and section area.

$$V_r = 0.182\sqrt{f_c}b_w d\left(1 + 0.07\frac{N}{A_c}\right) + \frac{A_{sw}}{s}f_y d \tag{2}$$

2.2 Capacity of the representative RC buildings

In order to obtain the capacity curves of the representative buildings, pushover analyses were performed and the base shear force and roof displacement relationship of the buildings was determined. During the analyses, the buildings were first subjected to gravity loads. Then, lateral force distribution was applied to each story level step by step and the capacity curves of the buildings were obtained. Lateral force distribution was obtained by multiplying each story weight and first modal shape amplitude at each story level. P–Δ effects were also considered in the analyses.

In Fig. 4, the plastic hinge formation of 5A and 5B buildings, at ultimate when the significant decay in lateral strength observed (see Fig. 5), is shown for readers to follow the discussions given in further paragraphs. In Fig. 5, the capacity curves of buildings 5A, 5B and 5C are plotted primarily for x and y directions. The vertical axis of the capacity curve represents the lateral strength ratio (V_y/W) obtained by proportion of the base shear force and the seismic weight of the building. The lateral axis of the capacity curve represents the global drift ratio obtained by proportion of the roof displacement capacity and building height (Δ/H).

As seen in Fig. 5, the lateral strength ratio of building 5A is around 10% in x direction while it is 18% in y direction. The pushover analysis results showed that all the columns reached their moment capacity at the lower and upper ends at the base story in x direction (Fig. 4a), but the lateral load capacity ratio of the building was calculated around 10% owing to lower moment capacities. However, the columns only reached their actual capacity at lower ends at the base story in y direction (Fig. 4b). This situation shows that the moment capacities of the columns are greater than those of beams (strong column-weak beam phenomenon). The maximum roof drift ratio of the building is obtained as 0.9 and 1.3% in x and y directions, respectively. Due to the insufficient confinement details of the structural members, the lower drift ratios are obtained for building 5A when compared with code-based constructed buildings.

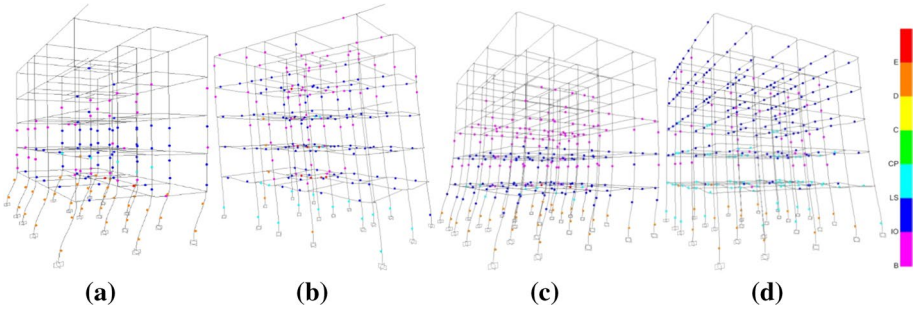

Fig. 4 Plastic hinge formation of buildings 5A and 5B in both principal directions. **a** 5A-x direction. **b** 5A-y direction. **c** 5B-x direction. **d** 5B-y direction

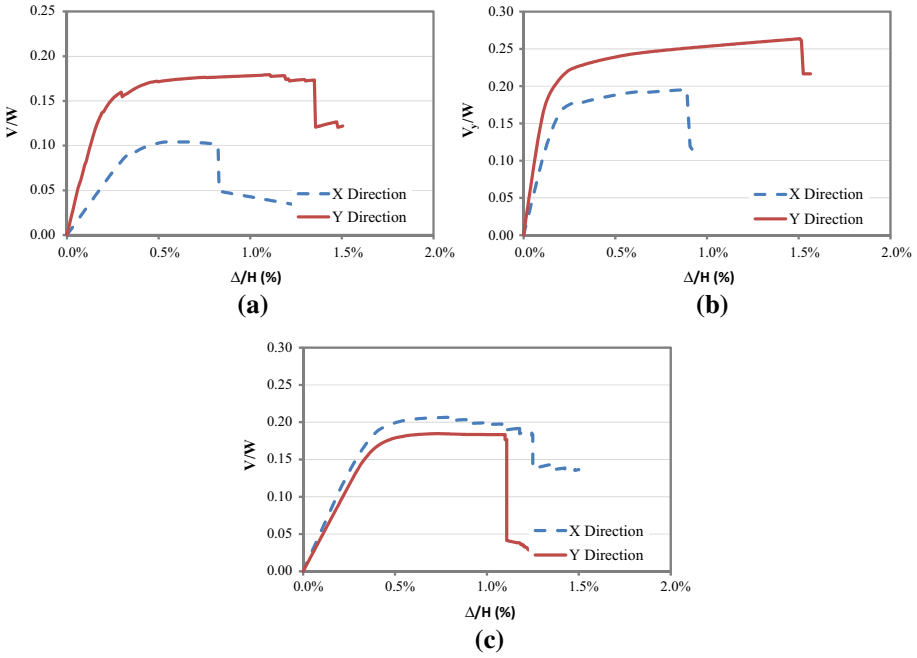

Fig. 5 Pushover curves for buildings 5A, 5B and 5C

The lateral strength ratio of building 5B is around 18 and 23% in x and y directions, respectively (see Fig. 5). When the floor plan of building 5B is inspected, it can be seen that the weak direction of the building is x direction. As well as in building 5A, the lower and upper ends of the columns reached their moment capacity in weak direction of building 5B (Fig. 4c). Furthermore, when the plastic hinge formation of principal y direction is checked (see Fig. 4d), it can be seen that only the lower ends of the columns are exceeded the yield level at the base story. In other words, the beams reached their moment capacity at the base story in y direction owing to the strong column-weak beam mechanism. In effect, this mechanism is preferred in design philosophy. However, lower moment values were obtained at the upper ends of the columns due to weak beams. Thus, this mechanism hindered the expectation of high capacity differences. The maximum global drift ratio is obtained as 0.88 and 1.5% in x and y directions, respectively.

Figure 5 clearly indicates that the lateral strength and global drift ratio of building 5C is relatively close in x and y directions. It was observed that the lateral strength capacity ratios were around 20 and 18% while the drift ratios were around 1.3 and 1.1% in x and y directions, respectively.

As can be seen from Fig. 5, depending on the structural characteristics, different capacity curves are obtained from the representative buildings. The studies of Inel et al. (2008) and Akkar et al. (2005c) also stated the observation of considerable differences between the capacity curves of mid-rise RC buildings. The reasons for such differences in the capacity curves were expressed and listed as the practice of constructing techniques, preliminary design, structural system characteristics, nonlinear behavior of structural mechanism and assumptions in the analysis models.

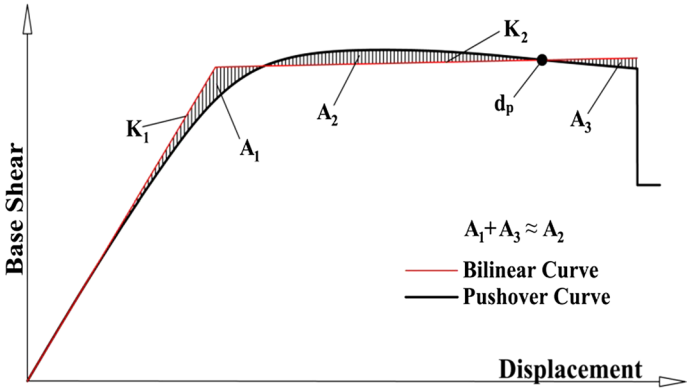

Fig. 6 Typical pushover curve and bi-linearization

Table 2 Dynamic properties of equivalent SDOF models for representative RC buildings

Building model	W (kN)	H (m)	Direction	T_1 (s)	K_2/K_1 (%)	α_1	Γ_1	Δ_y (m)	S_{ay} (g)
5A	8295.06	14.80	X	1.16	4.240	0.873	1.286	0.037	0.110
			Y	0.64	0.940	0.825	1.341	0.020	0.200
5B	11,587.75	14.70	X	0.63	1.264	0.893	1.253	0.020	0.200
			Y	0.47	1.159	0.866	1.273	0.142	0.258
5C	7625.19	14.00	X	0.77	0.150	0.794	1.323	0.036	0.245
			Y	0.86	1.520	0.794	1.324	0.041	0.225

2.3 Equivalent SDOF systems of RC buildings

After the pushover analyses, the capacity curves of the representative buildings were idealized by bilinear curves considering the ATC-40 guideline and the EUROCODE-8. Spectral acceleration (S_{ay}) and hence displacement (S_{dy}) at yield was approximated by the EUROCODE-8. The EUROCODE-8 approach was also utilized to equalize the areas under the actual curves and the idealized force–deformation curves. The ultimate displacement point (d_p) was determined by the equal displacement approximation suggested in the TEC-2007 and the EUROCODE-8. If the spectral displacement does not intersect the capacity curve then ultimate displacement of the buildings was attained when the significant decay in lateral strength was recorded. For this purpose, spreadsheet software which computes the dynamic properties of the building and performs iteration procedure to represent the bilinear behavior of the SDOF system was developed by the authors. In Fig. 6, typical and idealized (bilinear) capacity curves (slope before yield K_1 and post-yielding slope, K_2) are shown.

The dynamic characteristics of the equivalent SDOF systems were then calculated in accordance with the ATC-40 guideline (modal mass coefficient (α_1), modal participation factor (Γ_1), natural periods (T_1) and spectral quantities at yield and ultimate). In Table 2, yield displacement of equivalent SDOF models (Δ_y) and the dynamic properties of each

representative building for x and y directions are given. In addition, the seismic weights (W) and building heights (H) of the representative RC buildings are provided.

3 Selection of ground motion record sets

In modern seismic codes, time history analysis is accepted as one of the analysis methods for design and/or performance evaluation (TEC-2007, FEMA-368, EUROCODE-8, ASCE 07-05, GB). According to the required conditions of these codes for time history analysis, code-compatible ground motion records can be used if the average response spectrum of the selected ground motion records is compatible with the design acceleration spectrum within a stated period range. In the present study, the TEC-2007 compatible ground motion records sets are used for nonlinear time history analysis. During the analyses equivalent SDOF models are used and hysteretic behavior is considered as elasto-plastic with post-yield hardening effects. In addition, the damping ratio of the buildings is taken equal to 5%. Ground motion records are selected from the European Strong Motion Database (Ambraseys et al. 2004a). There are 2213 strong ground motion records available from 856 earthquakes recorded at 691 different stations in the database (Ambraseys et al. 2004b).

3.1 Design acceleration spectrum and time history analysis procedure defined in the TEC-2007

96% of Turkey's land is located on different seismic zones (1st, 2nd, 3rd, 4th, and 5th degree seismic zones) according to the current seismic hazard zoning map prepared by the Ministry of Public Works and Settlement (http://www.deprem.gov.tr/en/category/earthquake-zoning-map-96531). For the seismic hazard map of Turkey, the seismic zones were determined by using acceleration zonation map that had been calculated with the probabilistic method. It assumes that for ordinary buildings the probability of exceedance of the expected maximum acceleration within a period of 50 years is 10%. Thus, earthquake zones of Turkey are classified as follows due to expected acceleration values. In accordance with the TEC-2007 the design ground acceleration is 0.40, 0.30, 0.20 and 0.10 g for the 1st, 2nd, 3rd and 4th degree seismic zones, respectively. The 5th degree seismic zone is accepted as a non-seismic zone and the design ground acceleration is zero for this zone.

In the TEC-2007, structures are designed by 5% damped elastic design spectrum that can be defined as an earthquake level that has a 10% probability of exceedance in 50 years for buildings with the building importance factor $I=1$. The mathematical expression of this spectrum is given in Eq. 3. In Eq. 3, T_1 is the first natural vibration period of building in the direction of the earthquakes considered, T_A and T_B are the spectrum characteristic periods that depend on local soil classes defined in the TEC-2007, A_0 defines effective ground acceleration coefficient and I is the building importance factor ($I=1$ for residential and office buildings). Four local soil classes are defined in the TEC-2007: Z1, Z2, Z3 and Z4. The local soil classes for T_A and T_B are given in Table 3. Elastic spectral accelerations are calculated by multiplying $A(T_1)$ and *gravity* (g).

Earthquakes that cause serious loss of life and property in Turkey occur in the 1st degree seismic zone (Ilki and Celep 2012). In addition, the majority of Turkey's existing building stock is located in cities in this seismic zone. Thus, in this study, the 1st seismic zone is considered. The effective ground acceleration coefficient A_0, representing 1st degree seismic zone, is taken as 0.40.

Table 3 Spectrum characteristic periods for local soil classes

Local soil	T_A (s)	T_B (s)
Soil Z1	0.10	0.30
Soil Z2	0.15	0.40
Soil Z3	0.15	0.60
Soil Z4	0.20	0.90

$$A(T_1) = \begin{bmatrix} (A_0 I)\left(1 + 1.5\frac{T_1}{T_A}\right) & 0 \le T_1 \le T_A \\ (A_0 I)2.5 & T_A \le T_1 \le T_B \\ (A_0 I)2.5\left(\frac{T_B}{T_1}\right) & T_1 \ge T_B \end{bmatrix} \quad (3)$$

In Fig. 7, elastic spectral acceleration for local soil classes that would be used to determine seismic loads for the residential buildings, which are located in 1st degree seismic zone, are given.

In the TEC-2007, artificially generated, simulated or previously recorded ground motion records can be used to perform nonlinear time history analysis of buildings and building-like structures. Local site conditions should be appropriately considered in using recorded or simulated ground motions. At least three ground motion records should be used for time history analysis and the selected records should meet the following criteria:

- The duration of strong ground motions should be greater than 5 times the natural period of the building and should be longer than 15 s.
- The average of zero-period spectral acceleration values of the selected ground motion records shall not be less than $A_0 g$ for the buildings.
- The average of spectral acceleration values of the selected records shall not be less than 90% of the elastic spectral accelerations for the periods between $0.20T_1$ and $2.00T_1$ according to the first natural period of buildings T_1 for considered analysis direction.

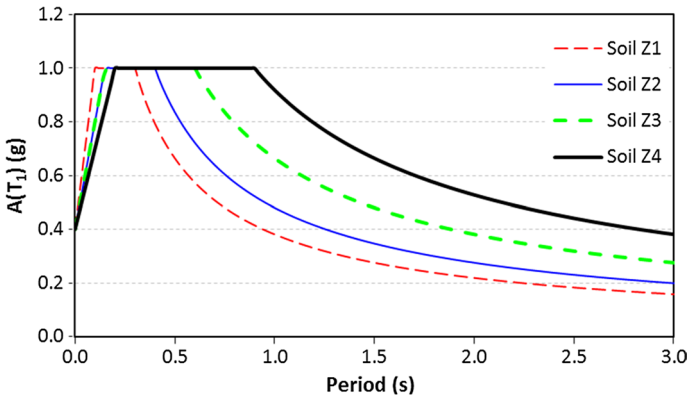

Fig. 7 Elastic spectral acceleration for local soil classes defined in TEC-2007

- The mean value of structural response from all of the analyses could be used if at least seven ground motion records are used; otherwise, the maximum value of structural response quantities should be used.

In addition to conditions described above, following additional criteria are considered during the obtaining of ground motion sets:

- In the TEC-2007, the lower limit of average spectral acceleration values of ground motion record sets is proposed as 90% of the elastic spectral acceleration, but the upper limit is not defined. In order to get more compatible results with the design spectra, the upper limit is also defined as 1.10. Accordingly, the average spectral acceleration value of ground motion record sets is limited between 0.90 and 1.10 of the elastic spectral acceleration for the periods between $0.20T_1$ and $2.00T_1$.
- The last criterion deals with the scaling factor used in scaling the amplitude of the original acceleration records. As known, the scaling factor plays a crucial role in the process and one prefers to keep modification of the original records to a minimum. In general, scale factors closer to unity are preferred and many ground motion experts recommend a limit on the amount of scaling applied (Watson-Lamprey and Abrahamson 2006). Recommended limits on scaling typically range from factors of 2–4 (Bommer and Acevedo 2004). In this study, the scaling factor was adapted to 0.50–2.00.

3.2 Ground motion data sets

In this study, for each considered local soil class, the ground motion record sets included in three different earthquake groups that have 7, 11 and 15 number of ground motion components are used to perform nonlinear time history analysis. Five ground motion record sets are used in each earthquake group.

In order to obtain code-compatible ground motion record sets, initially, the following criteria of epicentral distance (R), magnitude (M) and peak ground acceleration (PGA) are used to obtain a catalogue from the European Strong Motion Database (Ambraseys et al. 2004a): R is in the range of 10–50 km; M is greater than 5.5; and PGA is 0.10 g or higher. Afterwards, ground motion record sets are obtained through record selection from the catalogue. Considering the criteria, 542 horizontal components of 271 ground motion records are selected from the database for the catalogue.

These 542 horizontal components in the catalogue were grouped based on the local soil classes that they were recorded in. According to the EUROCODE-8 definition of local soil classes, there are 190 horizontal components of 95 ground motion records for soil class A; 236 horizontal components of 118 ground motion records for soil class B; and 116 horizontal components of 58 ground motion records for soil class C in the catalogue. It should be noted that there are very few ground motion records satisfying the abovementioned criteria about M, R and PGA in the database for soil class D and E. Thus, soil class D and E are ignored for the catalogue. Soil class Z1, Z2, and Z3 defined in the TEC-2007 are compatible with soil class A, B and C defined in the EUROCODE-8, respectively. Hence, in order to obtain record sets for Soil class Z1, Z2 and Z3, ground motion records recorded on soil class A, B and C, are considered, respectively.

For each soil class of Z1, Z2 and Z3, 15 ground motion record sets are obtained, considering that only those ground motion records are recorded in the matching soil class sites, i.e. on sites with the soil class A, B and C, respectively. Selection and scaling

ground motion records to match a given design spectrum can be formulated as an engineering optimization problem such that average square root of the sum of squares of the difference between the code-based response spectrum and average response spectrum of selected and scaled ground motions within a period range of interest (Naeim et al. 2004; Iervolino et al. 2008, 2010a). Required properties of ground motion records defined in seismic design codes can be considered as constraints of the optimization problems. When the selection and scaling problem defined and formulated as engineering optimization problem, several methods can be used for the solution. In this study, a solution model based on heuristic harmony search algorithm (Geem et al. 2001) is used to obtain ground motion record sets. The detailed information on the ground motion selection procedure used in the present study can be found in Kayhan et al. (2011) and Kayhan (2016). It should be noted that all the 45 ground motion record sets are compatible with the TEC-2007 and are also satisfying all the constraints considered in this study. Appendix A provides the label of ground motion components and the corresponding scale factors selected for all the ground motion record sets while Appendix B presents detailed information about the ground motion records.

Figure 8 illustrates the representative examples for compatibility between the mean spectra of the ground motion record sets and the target spectra. Figure 8a shows the individual response spectra (thin continuous lines) and the mean spectrum (thick continuous line) for Set 1 with 15 ground motion components, and the target spectrum for Soil Z2 (dashed line) can be shown. Figure 8b presents the mean spectra of five ground motion record sets with 15 ground motion components and the target spectrum for Soil Z2 can also be seen.

As can be seen from Appendix A, some horizontal components are in different ground motion record sets with different scale factors. For example, considering Soil Z1, "6333y" is selected in Set1 and Set2, "292y" is selected in Set4 and Set5 for the sets with 7 ground motion components and "369x" is selected in Set2, Set3 and Set4 for the sets with 11 ground motion components. However, it is not possible to say that some particular records are selected in many of the record sets. In addition, even if a ground motion component takes place in different record sets, it has different scale factors in each record set. Thus, code-compatible record sets used in this study are randomly selected, and they can be accepted to be independent from each other. There is a possibility of selecting the same records in different code-compatible sets, because

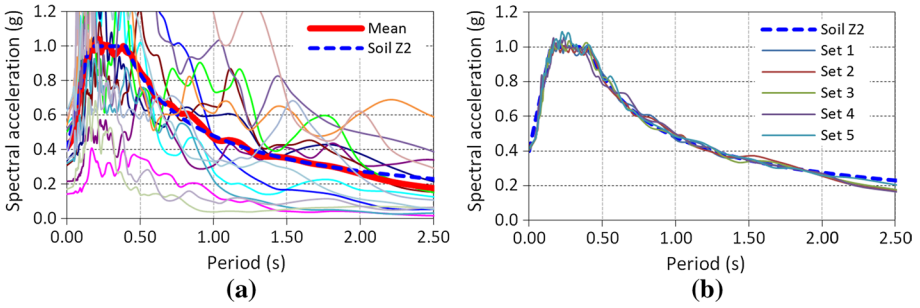

Fig. 8 Representative examples for compatibility between mean spectra of the record sets and target spectra defined in the TEC-2007. **a** The individual response spectra and mean spectrum for a set and target spectrum. **b** The mean spectra of the five record sets and target spectrum

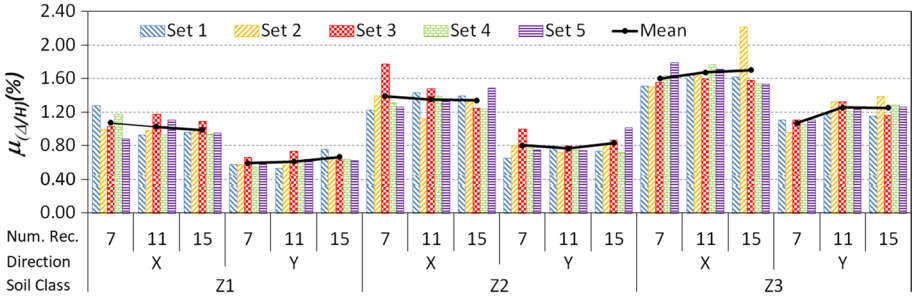

Fig. 9 $\mu_{\Delta/H}$ values of the record sets calculated for building 5A

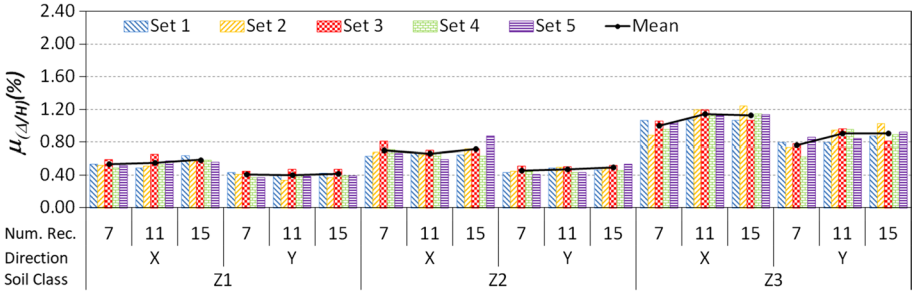

Fig. 10 $\mu_{\Delta/H}$ values of the record sets calculated for building 5B

this situation is related with the number of ground motion records in a catalogue and the record numbers in a ground motion sets. If the number of records in a catalogue increases, this possibility may decrease and vice versa.

4 Evaluation of dynamic analysis results

4.1 The mean of maximum drift ratio demands for ground motion record sets

In this part of the present study, the drift ratio demands obtained using ground motion records sets are statistically evaluated. For this purpose, the maximum global drift ratios (Δ_{max}/H) of the individual ground motions are determined from the nonlinear time history analysis of the buildings. As mentioned before, in order to make seismic design or performance evaluation, the mean of structural responses can be used if at least seven ground motion records are used for the time history analysis according to modern seismic codes such as the TEC-2007, EUROCODE-8, FEMA-368 etc. In this study, record sets with 7, 11 and 15 ground motion records are used. Hence, the mean ($\mu_{\Delta/H}$) of the Δ_{max}/H values of records is calculated for each record set.

It can be seen from the Figs. 9, 10 and 11 that the $\mu_{\Delta/H}$ values of buildings 5A, 5B and 5C, respectively are plotted according to the number of records, principal direction and soil class. It is worth reminding that for each number of records (7, 11 and 15) and soil class, five record sets are used. The $\mu_{\Delta/H}$ values of each record set can be seen from the figures

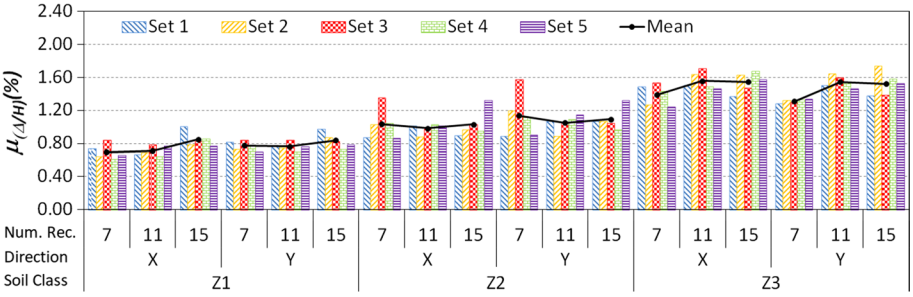

Fig. 11 $\mu_{\Delta/H}$ values of the record sets calculated for building 5C

with distinct colors. In addition, the mean of five $\mu_{\Delta/H}$ values are plotted for each number of records in the set, soil class, and analysis direction.

The $\mu_{\Delta/H}$ values of building 5A are given in Fig. 9 for each soil type. It can be seen from the figure that the mean of maximum drift ratios are different, although all obtained records sets are compatible with the target spectrum for the considered soil type. The figure clearly indicates that the mean drift ratios are increasing on average from Z1 to Z3 soil class. For example, the $\mu_{\Delta/H}$ values of the five sets with a number of seven records are 1.27, 0.99, 1.03, 1.18 and 0.88% for Z1 soil class and x direction. The average of these $\mu_{\Delta/H}$ values of the five sets is 1.07%. For Z2 and Z3 soil class, the averages of the $\mu_{\Delta/H}$ values of the five sets with seven records are 1.29 and 1.60% respectively. Vibration period of building 5A is $T_1 = 1.16$ s in x direction, As can be seen from Fig. 7, design spectral acceleration, $A(T_1)$, is minimum for Z1 and maximum for Z3. According to TEC-2007, the average spectrum of the record sets should be compatible with corresponding target spectrum in considered period range ($0.2T_1$–$2.0T_1$). Thus, average spectrum has smaller value for the record sets compatible with soil Z1 than the record sets compatible with soil Z2 and Z3 in this period range. In accordance with this situation, the mean drift ratio calculated for the record sets is the smallest for soil Z1 and the biggest for soil Z3. Furthermore, the increase in the number of records has no significant effect on the mean drift ratios of the record sets in any soil type. For example, the averages of the $\mu_{\Delta/H}$ values (for x direction) of the five sets with seven, eleven and fifteen records are 1.07, 1.02 and 0.99% respectively for Z1 soil class, and 1.39, 1.35 and 1.34% respectively for Z2 soil class.

Figures 10 and 11 present the $\mu_{\Delta/H}$ values calculated for buildings 5B and 5C, respectively. Similar observations stated for building 5A are also valid for buildings 5B and 5C. Similarly, the $\mu_{\Delta/H}$ values of code-compatible record sets are close to each other, the mean drift ratios are increasing on average from Z1 to Z3 soil class and number of records has no apparent effect on the drift ratio demands.

The outcomes of this part clearly express that the mean of the maximum drift ratios of different record sets compatible with the same target response spectrum may be close to each other, but can show slight changes. Therefore, it can be said that the mean of the structural responses considered for code-based seismic design and/or performance evaluation purposes will vary according to the ground motion records used. Reliability based approximation may provide benefits to take account of the dispersion in structural responses. This approximation requires the detailed statistical evaluations of structural responses and their dispersions according to local soil classes or the number of records used for time history analyses. Thus, not only the central tendency but also dispersion of the structural responses is needed. For this reason, the dispersion of structural responses and the relationship

between the dispersion and local soil classes and the number of records are investigated in the next section.

4.2 The dispersion of maximum drift ratio demands for ground motion record sets

In recent years, probability-based studies have become more prevalent (Lin 2008; Askan and Yucemen 2010; Mitseas et al. 2016; Kayhan and Demir 2016; Yamin et al. 2017) in the field of earthquake engineering. Probability-based seismic design or evaluation requires the knowledge of the probability distributions of seismic structural responses (e.g. maximum inter-story drift demand ratio) considered as random variables. In the cases in which the probability distributions of random variables cannot be precisely determined, the parameters of considered probability distribution are needed. For example, in addition to the mean (μ), there is also a need for a standard deviation (σ) which represents dispersion around the mean. One of the indicators of dispersion around the mean is the coefficient of variation (CoV), the ratio of the standard deviation to the mean. In order to evaluate the dispersion of Δ_{max}/H values in a record set around the mean of the same set $\mu_{\Delta/H}$, CoV_{Δ} is calculated for each ground motion record set.

In Fig. 12, CoV_{Δ} distribution of building 5A is plotted for each soil class. In addition, the mean of five CoV_{Δ} values are plotted for each number of records in the set, soil class, and analysis direction. As also shown by the figure, it can be said that dispersion of Δ_{max}/H values around the $\mu_{\Delta/H}$ is quite high for each record set. The lowest and highest values were determined to be 0.52 and 1.89, respectively. Obtained results imply that the dispersion is increasing with the increasing number of ground motions in the record sets even if they are compatible with the same target design spectrum.

CoV_{Δ} distributions of building 5B and 5C are separately illustrated in Figs. 13 and 14. In some record sets, CoV_{Δ} values are even higher than 2.0, especially for Z3 soil class and similar to building 5A, the dispersion of 5B and 5C buildings is also high for all considered soil classes and record sets. Dispersion of drift ratios increases with the increasing number of records in the record sets. CoV_{Δ} values get remarkably higher, especially for the Z3 classes and considered buildings.

It is a known fact that seismic codes especially focus on matching between target response spectrum and mean response spectrum of a record set within a certain period range, but they do not consider the compatibility between individual records and target response spectrum. In this case, for any period value in the considered period range, the scatter of spectral acceleration of the individual records (S_a) in the record set around the

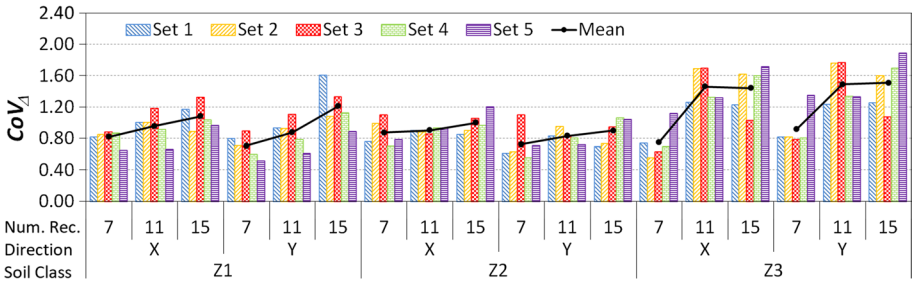

Fig. 12 CoV_{Δ} values of the record sets calculated for building 5A

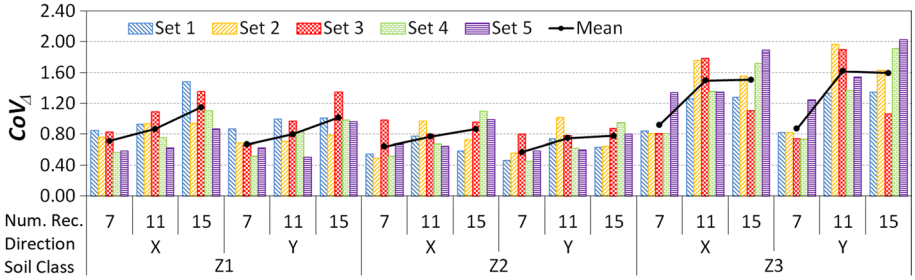

Fig. 13 CoV_{Δ} values of the record sets calculated for building 5B

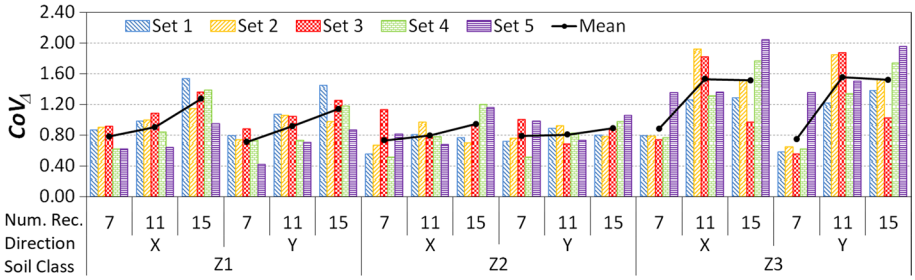

Fig. 14 CoV_{Δ} values of the record sets calculated for building 5C

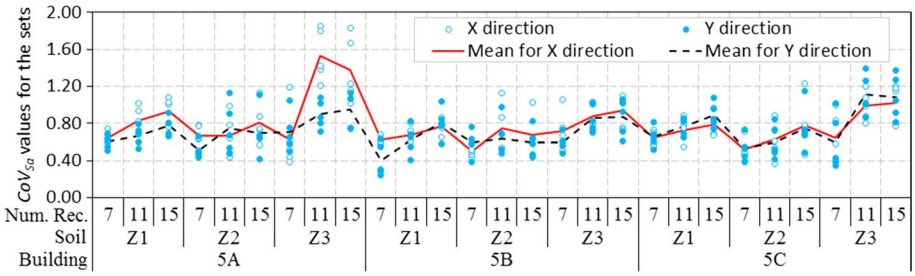

Fig. 15 CoV_{Sa} values of ground motion record sets

mean (μ_{Sa}) of the same record set cannot be controlled and high variations can be observed. Accordingly, the variations in Δ_{max}/H (or any structural response considered) values of individual records around the $\mu_{\Delta/H}$ of the record set can be high. For example, if the Set1 of Z2 soil class shown in Fig. 8 is considered, it can be seen that S_a values of 15 records range between 0.181 and 1.641 g at the period of 0.47 s that of the natural period of building 5B in principal y direction. At the period 0.47 s, spectral acceleration values of target spectrum and mean of record set are 0.879 and 0.898 g, respectively. It can be said that the mean of records sets and target spectrum spectral acceleration values have very good agreement, but dispersion of S_a values is very high. CoV_{Sa} value for this period is 0.57.

In Fig. 15, CoV_{Sa} values of the record sets are illustrated according to the local soil types and the number of records in the set for each building used in this study. As known, five record sets are considered for each soil class. The individual points in the figure represent CoV_{Sa} values calculated for each of the record sets. Continuous and dashed lines are

plotted to point the means of CoV_{Sa} values for x and y directions. It can be understood from the figure that the variations in $S_a(T)$ values are also very high.

In general, Fig. 15 implies that CoV_{Sa} values of ground motion sets are also higher than 0.4. If the continuous or dashed lines corresponding to the means of CoV_{Sa} values are followed, it is possible to say that CoV_{Sa} values are also increasing with an increasing number of ground motion records. For example, considering building 5A and soil Z1, the means of CoV_{Sa} are 0.65, 0.83, and 0.93 for x direction and 0.60, 0.67, and 0.72 for y direction, for the record sets with 7, 11 and 15 records, respectively. Besides, considering the building 5C, CoV_{Sa} values are increasing with an increasing number of records in a set for all the soil types considered. It can be said that a similar situation is observed in the building 5B except for the record sets that have 15 records for the Z2 soil class.

The results summarized in Figs. 12, 13 and 14 imply that the application of the current code-compatible requirements given in the TEC-2007 similar to the modern seismic codes around the world may cause high dispersions in terms of structural responses. A similar observation was reported by Iervolino et al. (2010b). Katsanos et al. (2010) also highlighted similar findings by using the Eurocode-8 compatible ground motion record sets.

In addition to the requirements given in the seismic codes, the other factor that causes high dispersion in structural responses may be the limited number of ground motion records in record catalogues. Ground motion record sets are selected from the pre-selected record catalogues by considering some specific criteria. If a catalogue with smaller number of real ground motion records is used, the variation of spectral acceleration values in the sets may larger. As mentioned earlier, the record sets used in this study for the soil classes Z1, Z2 and Z3 are selected by using a catalogue of 190, 236, 116 record components, respectively. According to Fig. 15, the CoV_{Sa} values of the record sets compatible with the soil Z3, which are obtained by selecting from the catalogue with lower number of record components, are higher. If you have a catalogue with limited number of real ground motion records with different compatibility with design spectrum, the use of the larger number of ground motion records for the sets may further increase of the variation of spectral acceleration values in the sets. If lower number of records is preferred, relatively more compatible records with design spectrum may be selected for a set. Thus, dispersion of spectral acceleration values may be lower. If the number of records is increased, relatively less compatible records with design spectrum may be added to set. In this case, dispersion of spectral acceleration values may increase. If the high dispersion of spectral acceleration values is the reason of the high dispersion of drift ratio demands, the dispersion of the drift ratio demands may further increase with the larger number of ground motions in the record sets.

4.3 One-way analysis of variance (ANOVA)

The results provided in Figs. 9, 10 and 11 indicate that the mean drift demands calculated for different ground motion record sets compatible with the same design spectrum are close to each other. Thus, it can be said that the mean drift demand calculated for a building is a random variable which depends on the record sets used for the time history analysis. In order to evaluate the differences between the mean drift demands of five ground motion record sets for each building and principal analysis direction, one-way analysis of variance (ANOVA) is used. Each local soil type and the number of ground motion record in a set are also separately considered for one-way ANOVA. One-way ANOVA is used to determine whether there is any statistically significant difference between the means of three or more independent samples using the F-test (Gamst et al. 2008).

The null hypothesis for one-way ANOVA refers to that the means of all populations are equal for c independent samples that have normally distributed k size members [Eq. (4)]. In order to test the null hypothesis, the source of two variations: the variation between sample means (*SSA*) and the variation within samples (*SSW*) should be calculated. Mathematical expressions of sum of squares among (*SSA*) and sum of squares within (*SSW*) are given in Eqs. (5) and (6). Total variation is the sum of *SSA* and *SSW*. In the equations, c is the number of samples, k_j and μ_j define the member size and the mean of sample j, respectively, and μ_{all} is the mean of all samples, while X_{ij} refers to the *ith* member of sample j.

$$H_0 : \mu_1 = \mu_2 = \mu_3 = \cdots = \mu_c \tag{4}$$

$$SSA = \sum_{j=1}^{c} k_j \left(\mu_j - \mu_{all}\right)^2 \tag{5}$$

$$SSW = \sum_{j=1}^{c} \sum_{i=1}^{k} \left(X_{ij} - \mu_j\right)^2 \tag{6}$$

The degrees of freedom between samples are calculated by $c-1$ while those within samples are calculated by $n-c$. To calculate the degrees of freedom within samples, n, the sum of member sizes of all samples is needed. Afterwards, two variances, the mean squares between samples (*MSA*) and within samples (*MSW*) are calculated by using Eqs. (7) and (8). Lastly, the F statistic, simply a ratio of two variances, is determined by taking the ratios of *MSA* and *MSW*.

$$MSA = \frac{SSA}{c-1} \tag{7}$$

$$MSW = \frac{SSW}{n-c} \tag{8}$$

F value is mostly illustrated by using a tabular format shown in Table 4. Finally, F value is compared with F-critical value. F-critical value is upper critical value of the F distribution with the significance level (α) and degrees of freedom within samples ($n-c$) and between samples ($c-1$). Significance level is used to represent the value of an F-critical value having cumulative probability of ($1-\alpha$) and mostly taken equal to 5%. If the F value is smaller than the F-critical value, null hypothesis (H_0) is accepted.

In this study, five different record sets are used for each considered local soil class and number of ground motion records in a set. Thus, $c=5$. However, n, the sum of member

Table 4 Typical representation of one-way ANOVA table

Source of variation	Sum of squares (*SS*)	Degrees of freedom (*df*)	MS (*Variance*)	Computed F
Among samples	*SSA*	$c-1$	*MSA*	$F = \frac{MSA}{MSW}$
Within samples	*SSW*	$n-c$	*MSW*	
Total	*SSA* + *SSW*	$n-1$		

sizes of all samples, varies with the number of ground motions in a record set. For the record sets with 7, 11 and 15 ground motion records, n is 35, 55 and 75, respectively. Thus, considering $\alpha = 0.05$, the F-critical value for the record sets with 7, 11 and 15 groups are 2.690, 2.557 and 2.503, respectively. The F values calculated for each building, principle direction, local soil class and the number of ground motion records in a set are plotted in Fig. 16.

The figure demonstrates that the highest F value is calculated as 0.576 and the corresponding F-critical value is 2.690. Thus, H_0 is accepted. In other words, the drift demands obtained by using five ground motion record sets that are compatible with the same design spectrum are drawn from the populations with an equal mean at the 95% confidence level. The lower value of F indicates that the effect of variability within samples (MSW) due to the random causes on the total variability is larger than the effect of variability between samples due to the differences between the mean of samples. Thus, the differences between the mean of samples are accepted statistically insignificant considering the results of one-way ANOVA. According to the F-values given in Fig. 16 and the corresponding F-critical values, H_0 is also accepted for the other buildings, local soil types and the number ground motion records sets examined in this study.

One-way ANOVA results have demonstrated that the mean drift demands of different ground motion record sets which are compatible with a particular design spectrum can be treated as they are random samples of the same populations. In this case, some conclusions can be drawn about the distribution of populations by using relevant drift demands.

In order to make a seismic design or evaluation, mean structural responses can be used according to modern seismic codes. However, it should be noted that randomly changing structural responses may be obtained for each ground motion record sets compatible with the considered design spectrum. Thus, it would be useful to obtain data on the distribution of mean structural responses. It can be useful to use an interval of mean structural responses for a particular confidence level. Furthermore, dispersion of structural responses should also be taken into consideration for a reliability based seismic design or evaluation.

4.4 Sampling distributions of mean drift demand ratios

Sampling distribution can be defined as the distribution of a statistic for all possible samples taken from the same population. It is derived from a random sample of size n. Thus,

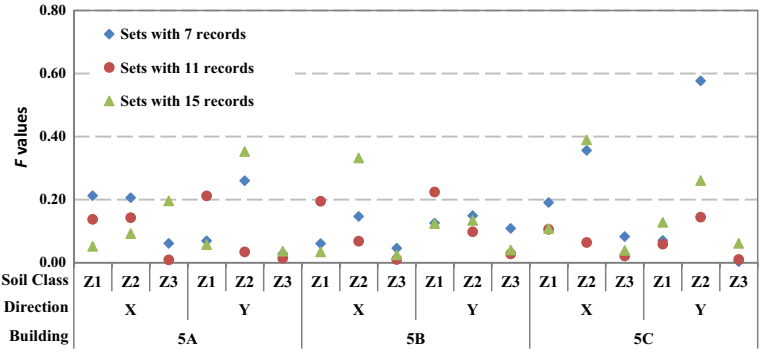

Fig. 16 F values calculated for considered buildings and local soil classes

the sampling distribution of a statistic depends on the sample size and the sampling procedure. Sampling distributions can be characterized by two important statistics: sample mean (m) and the sample variance $Var(m)$. The sampling distribution of the mean, namely the probability distribution of mean (m), represents the variability of sample means m around the population mean μ.

In this study, considering the prescribed degree of confidence within which the population parameters μ lie, interval estimates of drift demand ratios are calculated. For the population parameter μ, the probability statement of the interval estimates can be given as follows in Eq. 9:

$$P(l \leq \mu \leq u) = 1 - \alpha \quad 0 < \alpha < 1 \tag{9}$$

In Eq. 9, l and u donate the lower and upper confidence limits, respectively. l and u depend on the numerical value of the sample mean m for a particular sample. The $1-\alpha$ is defined as the confidence coefficient. The interval (l, u) refers to the $100(1-\alpha)\%$ confidence interval for the parameter μ. The quantity $100(1-\alpha)\%$ is the confidence level of the interval.

For a random sample of n observations taken from a normally distributed population with the mean μ and the variance σ^2, the value of the sample mean m is calculated by using the values of the random variables in the sample. In this case, m is also a random variable. It is expected that the sample mean m is centered about the population mean μ, but its dispersion decreases when the sample size increases (Eq. 10).

$$E[m] = \mu \quad \text{and} \quad \text{Var(m)} = \frac{\sigma^2}{n} \tag{10}$$

Considering a large sample of size n from a population with the mean μ and the variance σ^2, the Central Limit Theorem specifies that sample distribution is normal even if the population does not come from a normal distribution and the sample mean m will be equal to population mean (μ) and variance can be calculated by the proportion of population variance and sample size (σ^2/n). If the sample size is small, the Student's t distribution can be used to calculate the confidence intervals of population mean μ. For a random sample of size n and $100(1-\alpha)\%$ confidence interval, interval estimates of μ are given by Eq. 11. In Eq. 11, $t_{\alpha/2,n-1}$ is the upper $100\alpha/2$ percentage point of the t distribution with $n-1$ degrees of freedom and $s/\sqrt{n}$ is the standard error of sample means.

$$m - t_{\alpha/2,n-1}\frac{s}{\sqrt{n}} \leq \mu \leq m + t_{\alpha/2,n-1}\frac{s}{\sqrt{n}} \tag{11}$$

In practice, confidence intervals are mostly taken as 90 or 95% confidence level. In this study, 90% confidence level is used for representative calculation. It should be noted that one can use any confidence level and corresponding confidence limits for a specific seismic design and/or an assessment study.

The 90% confidence intervals (l, u) for the mean of the populations of drift demand ratios ($\mu_{\Delta/H}$) are calculated for each building, analysis direction, local soil class and the number of records in a set. As mentioned before, five different ground motion sets are used for each local soil class and considered number of ground motion records in a set. Hence, n is taken equal to 5 and the corresponding $t_{\alpha/2,n-1}$ is calculated as 2.13 for the corresponding confidence interval of the population means.

The central tendency of sample means of drift demand ratios ($\bar{m}$) are given in Fig. 17. As shown in the figure, $\bar{m}$ values vary with the building and analysis directions considered,

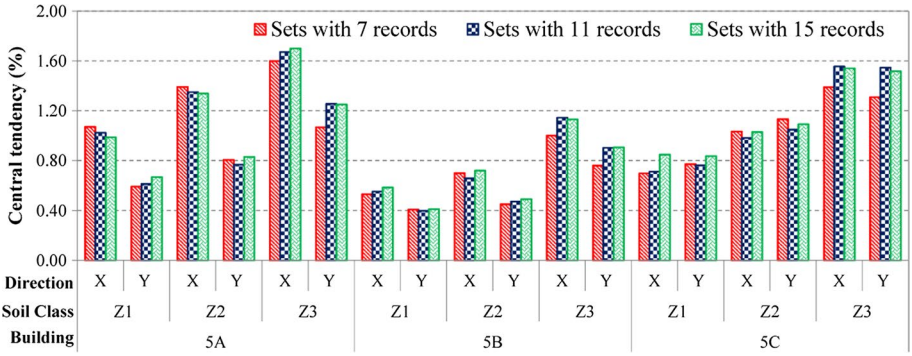

Fig. 17 Central tendency of sample means $\bar{m}$ (%)

and increase if the soil class changes from Z1 to Z3. For example, for the building 5A and the ground motion record sets with 7 records, the value of $\bar{m}$ is 1.18% for soil Z1, 1.38% for soil Z2 and 1.64% for soil Z3 considering X direction. For the same building and the record sets, the value of $\bar{m}$ is 0.69, 0.93 and 1.14% in Y direction for the Z1, Z2 and Z3 soils, respectively. In Fig. 17, the values of $\bar{m}$ vary randomly with the number of ground motion records in record sets, but they are relatively close to each other. For example, for the building 5B and soil class Z1, the value of $\bar{m}$ in X direction is 0.62, 0.55 and 0.61%, in Y direction it is 0.47, 0.40 and 0.45% for the record sets with 7, 11 and 15 ground motion records, respectively. It can be said that there is no significant effect of the number of ground motion record sets in record sets on $\bar{m}$ values, Table 5 displays the 90% confidence interval (l, u) of the mean drift demand ratios of the populations ($\mu_{\Delta/H}$) together with the relevant $\bar{m}$ values.

According to the Table 5, for the building 5A, soil Z1 and direction x, the confidence interval of $\mu_{\Delta/H}$ is (0.922, 1.220%) for the sets with 7 records, (0.917, 1.131%) for the sets with 11 records and (0.926, 1.048%) for the sets with 15 records. These confidence intervals indicate that if different ground motion record sets compatible with design spectrum for the soil class Z1 were used for the nonlinear time history analysis of the building 5A in direction x, the calculated mean drift demands ($\mu_{\Delta/H}$) of the records sets would be between the abovementioned lower and upper confidence limits with a 90% probability.

5 Conclusions

In this study, the global drift ratio demands obtained by nonlinear time history analysis using different code-compatible real ground motion record sets are statistically evaluated and the effect of the number of ground motion record sets is investigated. Three mid-rise RC buildings, representing the existing mid-rise buildings in Turkey, are selected and the drift ratio demands calculated for the selected buildings are evaluated in terms of mean and dispersion. The ground motion record sets compatible with the design spectra defined for local soil classes in TEC-2007 are considered. For each local soil class, five different ground motion record sets with 7, 11 and 15 ground motion records are used. The key observations and findings of this study are briefly summarized as follows:

Table 5 90% confidence intervals (l, u) for $\mu_{\Delta/H}$ (%)

Record number	Soil class	Direction	Building 5A			Building 5B			Building 5C		
			$\bar{m}$	l	u	$\bar{m}$	l	u	$\bar{m}$	l	u
7	Z1	X	1.071	0.922	1.220	0.533	0.498	0.567	0.697	0.608	0.787
		Y	0.594	0.553	0.635	0.408	0.372	0.444	0.772	0.717	0.827
	Z2	X	1.392	1.179	1.605	0.699	0.631	0.766	1.033	0.846	1.220
		Y	0.805	0.685	0.925	0.452	0.414	0.489	1.133	0.866	1.400
	Z3	X	1.600	1.486	1.715	1.001	0.928	1.075	1.390	1.263	1.517
		Y	1.067	1.005	1.129	0.760	0.677	0.844	1.310	1.289	1.330
11	Z1	X	1.024	0.917	1.131	0.553	0.490	0.615	0.711	0.650	0.772
		Y	0.613	0.539	0.687	0.398	0.353	0.444	0.763	0.713	0.813
	Z2	X	1.350	1.218	1.483	0.657	0.619	0.696	0.981	0.925	1.038
		Y	0.766	0.733	0.800	0.473	0.440	0.506	1.049	0.957	1.141
	Z3	X	1.672	1.608	1.736	1.145	1.096	1.194	1.556	1.454	1.658
		Y	1.256	1.191	1.321	0.903	0.831	0.974	1.547	1.477	1.617
15	Z1	X	0.987	0.926	1.048	0.586	0.555	0.618	0.848	0.757	0.939
		Y	0.667	0.617	0.716	0.412	0.374	0.450	0.836	0.749	0.924
	Z2	X	1.339	1.238	1.440	0.719	0.628	0.811	1.029	0.870	1.188
		Y	0.830	0.717	0.944	0.492	0.457	0.527	1.092	0.967	1.218
	Z3	X	1.700	1.422	1.979	1.131	1.064	1.198	1.542	1.424	1.659
		Y	1.250	1.159	1.341	0.907	0.833	0.981	1.518	1.373	1.663

1. The dispersion of the maximum drift ratio demands in a record set is quite high and as a result of investigations, it is suspected that the limited number of records in the catalogues, where the ground motion records are selected, could lead to high variability in drift ratio demands. In this study only one strong ground motion database (Ambraseys et al. 2004a, b) is used. Nowadays, many databases including a large number of strong ground motion records are also available such as Engineering Strong Motion (Luzi et al. 2016) and PEER Strong Motion Database (Ancheta et al. 2014). Using one or more of these databases this variability can be lowered. Moreover, results demonstrated that the variations of Z3 soil which have lower number of ground motion records in the catalogue is specifically higher. It is also possible to say that the dispersion of drift ratio demands increase proportional to the number of ground motion records in a record set. This result is valid for a wide range of vibration periods between 0.46 and 1.16 s which represent the first-mode dominated mid-rise RC buildings.
2. Observations have also shown that there is not a particular effect of the number of ground motion records (record set which have more than seven records) on the mean drift ratio demands. Thus, use of at least seven records seems adequate and practical for the design and evaluation practices.
3. Results obviously showed the possibility of obtaining distinct mean drift ratio demands for different record sets which have same number of records (e.g. 5 different record sets which have 7 records or higher) although they are compatible with the same design spectrum.
4. In order to explain variability of mean drift ratio demands for different ground motion record sets, one-way ANOVA is used. Although there is a clear variability among the record sets, ANOVA results demonstrated that mean drift ratio demands of different

ground motion record sets still can be accepted that they are random samples drawn from the same population at 95% confidence level.

5. In the light of ANOVA results, it can be deduced that instead of certain value, reliability based strategies should be used for the design or performance evaluation purposes. For this reason, sampling distribution technique is used to provide lower and upper bounds of mean drift ratio demands for a certain level of confidence. In this study, the confidence level was taken equal to 90% as a representative calculation and results indicated that different lower and upper bounds may be obtained for the mean drift ratio demands. On the other hand, what is more important is that it is monitored that in average, $\pm 10\%$ of the mean drift ratio demands can be assumed as the lower and upper bounds.
6. Modern seismic codes only concentrated on the compatibility between the target design spectrum and the average response spectrum of ground motion records in a record set within a certain period range. However, the compatibility between the individual response spectra of the records and the target spectrum is overlooked. In this case, the variation of the spectral acceleration of individual records for any period value in the period range cannot be controlled and high variations may be observed. Accordingly, spectral acceleration values and hence drift ratio demands of the three representative buildings have showed high variation in different vibration periods. In order to reduce the variation of the spectral acceleration in a set the additional criterion or recommendation about the compatibility between the individual acceleration spectra of the records and the target spectrum may be an effective option. This option may be adopted for a specific vibration period (for example effective initial period of the structure) and/or a specific period range (for example lower and upper period value relevant to effective period of the structure).

The definitions of time history analysis in modern seismic codes such as the TEC-2007, EUROCODE-8, FEMA-356, ASCE 07-05, GB 2010 are similar with some minor exceptions. For example, uniform hazard spectrum is used to define seismic hazard considering the local soil conditions and a certain number of ground motion records are required for time history analysis. In addition, matching is required between the design spectrum and the average response spectrum of the used ground motion records. In this study, TEC-2007 compatible ground motion record sets are used for the time history analysis. Considering the similarities in the definitions of time history analysis, it can be said that similar results may be obtained by using one of the above mentioned seismic codes.

It is worth stating that seismic demands of buildings mainly affected from lateral strength, natural period and post yielding effects. As selecting and scaling procedures of seismic codes initially take into account of demand estimation for performance evaluation, lateral strength and structural period play decisive role on the demands. For this reason, the results of the recent studies about evaluation of the code-based selection procedures may depend on the structures considered. On the other hand, the results of the present study indicate that the variability in structural responses should be considered in more detail for seismic design and/or performance evaluation. Reliability based approaches and/or stochastic distribution models seem to be appropriate tools to handle such issues numerically in the future studies. For this purpose, various structural configurations covering single or multiple degrees of freedom with various ground motion record set options covering larger number of records in record sets or large number of record sets may bring more powerful insights to the selection and scaling procedures in the future for seismic codes.

Appendix A1

See Table 6.

Table 6 Ground motion record sets with 7 ground motion components

Soil class	Set 1		Set 2		Set 3		Set 4		Set 5	
	Record	Scale	Record	Scale	Record	Scale	Record	Scale	Record	Scale
Soil Z1	6333y	1.626	369x	1.622	6331y	0.811	6278y	0.619	6269y	0.550
	410x	1.850	5272x	0.570	6262x	1.250	7158y	1.211	368y	0.587
	6278x	0.512	638y	1.131	6100y	1.939	646x	0.769	6331y	1.382
	412x	0.504	6333y	1.464	6341x	0.833	6333x	2.000	362x	1.535
	642x	0.847	6265x	0.737	383y	1.739	292y	0.870	604x	1.715
	1891y	1.998	603y	1.899	243y	1.399	6270y	0.816	6337x	1.638
	638x	0.805	6100y	1.729	292x	1.228	6331x	1.123	292y	1.228
Soil Z2	129x	1.043	6144x	0.737	645y	1.556	6496y	1.439	49x	0.621
	759x	0.839	760x	1.768	532y	0.870	1996x	1.398	645y	1.660
	572y	1.095	620y	0.832	6496y	1.762	946x	1.953	129x	1.000
	1984x	1.282	572y	1.179	7067x	1.449	548x	1.077	1984x	1.336
	645y	1.449	1984x	0.807	572y	1.111	352y	0.950	7257x	0.685
	1881x	0.918	630y	0.770	352y	1.433	595x	1.236	946x	1.902
	6138y	0.999	352y	1.197	946x	0.694	759x	0.500	6499x	1.376
Soil Z3	7010x	1.410	6978y	0.889	6606y	1.286	1230x	0.546	1230y	0.588
	644y	0.643	1230x	0.509	360x	1.030	141x	1.237	601x	1.055
	1230x	0.634	439y	0.517	1230x	0.623	375y	0.710	6962y	1.001
	141x	1.873	141y	1.573	6978y	0.968	6978y	1.171	6960x	1.977
	374y	1.031	6962x	1.705	6962x	1.940	6962x	1.979	375y	1.200
	6978y	0.972	360x	1.264	375y	0.679	648y	0.594	1959y	0.728
	6606y	1.189	555x	1.384	141x	1.867	360x	1.377	6962x	1.602

Appendix A2

See Table 7.

Table 7 Ground motion record sets with 11 ground motion components

Soil class	Set 1		Set 2		Set 3		Set 4		Set 5	
	Record	Scale	Record	Scale	Record	Scale	Record	Scale	Record	Scale
Soil Z1	383x	0.639	385x	1.034	6331y	1.475	5271x	1.590	642x	0.661
	6272x	0.933	467x	1.809	292x	1.207	646y	1.364	6342x	0.635
	6327y	1.750	5272y	1.506	621x	0.800	6265y	1.326	6337x	1.189
	5270x	1.131	369x	0.837	6269x	1.308	383y	0.535	410x	1.470
	4678x	1.111	628x	0.732	292y	0.735	369x	1.379	292x	0.976
	605y	0.540	1243x	0.755	6341x	1.144	6272x	1.564	6327x	0.913
	638x	0.637	6269y	0.876	369x	0.676	960y	1.152	1891y	1.577
	7158x	1.140	6336y	1.213	382x	1.118	6333y	1.114	604y	1.486
	359x	0.871	467y	0.711	6269y	1.149	6262y	1.217	626x	0.749
	369y	1.075	6331x	1.604	646y	1.330	6100y	1.388	362x	1.578
	6331y	0.845	6100x	0.624	6265y	0.724	638x	0.512	292y	1.026
Soil Z2	244y	1.381	129x	0.662	6138y	0.654	946x	1.373	7161x	0.877
	1720y	1.738	1720y	1.822	6138x	1.361	474x	1.004	6138x	0.520
	946y	0.807	595y	1.046	645y	1.185	572y	0.588	548y	0.841
	620x	0.788	293x	0.645	1720x	1.487	760x	0.665	5798y	0.952
	572x	1.838	5273x	0.606	129x	0.985	1720y	0.753	1887x	0.713
	645y	1.012	7257x	0.600	572y	1.529	142y	1.568	759x	1.084
	6145y	1.728	7155y	0.511	5798y	0.934	761y	0.828	1984x	0.550
	352y	1.254	760x	1.329	946y	1.489	1996x	1.833	549y	1.170
	1720x	0.505	1713y	0.984	352y	0.754	6329y	1.567	595y	0.992
	760x	1.853	142y	0.686	7257x	1.060	244y	1.101	352y	1.238
	1859y	0.738	247y	0.712	381x	1.105	352y	1.273	630y	1.011
Soil Z3	151x	0.778	7010x	0.563	1230y	1.032	950x	0.754	1959y	1.084
	601y	1.146	1230y	1.073	6962x	1.444	643y	1.932	555x	1.881
	1908y	0.752	151x	0.721	4477x	0.538	601y	1.080	360x	1.233
	141x	0.580	6975y	0.778	151x	1.348	643x	0.570	950x	0.636
	6978y	0.512	374y	0.722	6960x	1.311	6962y	1.540	601y	1.179
	6975y	1.408	6962x	1.099	375y	0.610	360x	1.547	151x	0.974
	648x	0.694	531x	1.881	360y	0.654	375y	1.377	141x	1.248
	360y	0.643	648x	0.646	6446y	1.641	6962x	0.549	375y	0.982
	7010y	0.936	601y	0.629	643y	0.851	1230x	0.678	1230y	0.808
	1230y	0.688	6446y	1.736	555x	1.474	1230y	0.753	360y	0.556
	360x	1.031	643y	0.817	601y	1.011	531y	1.005	6975y	0.649

Appendix A3

See Table 8.

Table 8 Ground motion record sets with 15 ground motion components

Soil class	Set 1		Set 2		Set 3		Set 4		Set 5	
	Record	Scale	Record	Scale	Record	Scale	Record	Scale	Record	Scale
Soil Z1	292y	1.282	4557x	1.080	412y	1.335	385y	0.844	960y	1.079
	598x	0.982	140y	1.408	6269y	1.669	369x	1.306	6262y	0.933
	6267y	0.739	6337x	1.139	292x	1.161	243x	0.763	6342y	0.743
	646x	1.393	605x	1.149	6342y	1.142	607y	0.895	382y	1.900
	646y	1.902	383x	0.959	1707y	0.762	382x	1.750	362y	1.356
	6269y	1.000	628y	0.710	652x	0.778	6337y	1.377	362x	1.096
	246y	0.714	6761y	0.780	382x	1.627	650x	1.026	140y	0.910
	7158x	0.655	6341y	0.753	369x	1.550	6761y	0.517	140x	0.628
	6331y	0.715	6331y	1.416	5271x	1.768	140y	0.945	412y	0.595
	652x	0.839	4679y	0.991	173y	0.811	467y	1.985	6269y	1.687
	412y	1.900	412y	1.202	603y	0.699	294y	0.690	6331y	1.536
	382x	1.767	6342y	0.528	6337y	1.403	6272y	0.685	6269x	1.630
	1707y	0.899	243y	1.565	628x	0.740	292x	0.792	6272y	1.344
	604y	0.763	292y	0.777	646y	0.841	243y	1.471	604x	0.767
	6341y	0.982	385y	0.750	764x	0.607	6331x	1.461	621x	0.738
Soil Z2	1720y	0.878	474x	1.310	502y	1.968	6138y	1.249	142y	0.937
	435x	0.677	6145x	0.770	6144y	0.697	572x	0.515	1881x	0.592
	7067x	1.101	572y	1.902	381x	1.549	49x	1.605	645y	1.238
	572x	1.275	6499x	1.584	6138y	1.737	502y	1.619	620x	1.342
	6138x	0.632	946x	1.519	142x	0.883	6444x	1.568	1735x	1.194
	6144x	1.188	352y	1.084	352y	1.201	1711x	0.869	760x	1.435
	760x	1.543	6964x	0.506	211x	0.871	620y	0.535	1245x	1.172
	645y	1.436	6422x	1.663	1720y	0.701	1720y	0.650	502y	1.149
	572y	0.760	5798y	1.362	548x	1.362	1984x	0.987	1984x	1.894
	352y	1.252	760y	1.181	6444x	1.640	7067y	0.987	352y	1.663
	6499x	1.233	6138y	1.705	1984x	1.387	1713y	0.679	627y	1.304
	49x	0.931	645y	1.348	7067x	1.120	6496x	0.806	1720x	1.080
	6422x	1.502	1314y	0.554	1720x	1.825	5273x	0.592	548x	0.882
	6444x	1.244	6496y	0.960	760x	1.094	760x	1.229	5798y	1.069
	946x	1.806	6445y	0.598	142y	0.659	352y	0.858	6138x	1.364

Table 8 (continued)

Soil class	Set 1		Set 2		Set 3		Set 4		Set 5	
	Record	Scale	Record	Scale	Record	Scale	Record	Scale	Record	Scale
Soil Z3	643x	0.983	6962x	0.947	601y	0.749	360x	1.814	6962y	0.789
	379x	0.950	360x	1.519	141x	1.815	648x	0.657	379y	1.172
	374y	1.182	6975y	0.528	1230x	0.667	637y	0.534	601y	0.675
	151x	0.748	360y	0.892	648x	0.882	555x	0.660	151x	0.749
	648x	0.609	141x	0.509	1908y	0.944	6962x	1.745	6446y	0.647
	1230x	0.729	7010y	1.432	6962y	1.021	151x	1.488	170x	0.686
	1230y	0.790	601y	0.889	6975y	0.751	643x	1.397	375y	1.290
	643y	1.492	1230y	0.539	360x	1.796	643y	1.582	1959x	0.622
	1908y	0.560	648x	0.582	1230y	0.622	601y	1.062	1230y	1.214
	6975y	0.675	1230x	0.873	6978y	0.829	555y	1.621	6963x	0.506
	602x	0.752	6446x	0.709	643x	0.947	633y	0.628	648x	0.642
	360x	1.484	1257y	0.600	375y	0.769	7010y	1.999	141x	1.931
	373x	0.533	6963x	0.711	151x	1.029	6975y	0.990	6975y	1.011
	6962y	1.458	555x	1.379	379y	0.564	1230y	1.098	555y	0.697
	6960x	0.852	643y	1.710	7010y	0.780	1908x	0.527	360x	1.167

Appendix B

See Table 9.

Table 9 Detailed information about ground motion records selected for the record sets

Record	Earthquake	Date	M	Station	Record	Earthquake	Date	M	Station
49-X	Friuli	06/05/76	6.5	ST14	761-Y	Umbria Marche (aftershock)	14/10/97	5.6	ST265
129-X	Friuli (aftershock)	11/09/76	5.5	ST28	764-X	Umbria Marche	26/09/97	6.0	ST266
140-X	Friuli (aftershock)	15/09/76	6.0	ST36	946-X	Potenza	05/05/90	5.8	ST103
141-X	Friuli (aftershock)	15/09/76	6.0	ST12	950-X	Sicilia-Orientale	13/12/90	5.6	ST288
142-X	Friuli (aftershock)	15/09/76	6.0	ST14	960-Y	Sicilia-Orientale	13/12/90	5.6	ST296
151-X	Friuli (aftershock)	15/09/76	6.0	ST33	1230-X	Izmit	17/08/99	7.6	ST576
170-X	Basso Tirreno	15/04/78	6.0	ST46	1243-X	Izmit (aftershock)	13/09/99	5.8	ST575
173-Y	Basso Tirreno	15/04/78	6.0	ST49	1245-X	Izmit (aftershock)	13/09/99	5.8	ST598
211-X	Montenegro (aftershock)	15/04/79	5.8	ST67	1257-Y	Izmit	17/08/99	7.6	ST772
243-X	Valnerina	19/09/79	5.8	ST82	1314-Y	Ano Liosia	07/09/99	6.0	ST1101
244-Y	Valnerina	19/09/79	5.8	ST83	1707-Y	Duzce 1	12/11/99	7.2	ST1252
246-Y	Valnerina	19/09/79	5.8	ST61	1711-X	Ano Liosia	07/09/99	6.0	ST1255
247-Y	Valnerina	19/09/79	5.8	ST279	1713-Y	Ano Liosia	07/09/99	6.0	ST1257
292-X	Campano Lucano	23/11/80	6.9	ST98	1720-X	Dinar	01/10/95	6.4	ST543
293-X	Campano Lucano	23/11/80	6.9	ST99	1735-X	Adana	27/06/98	6.3	ST581
294-Y	Campano Lucano	23/11/80	6.9	ST100	1859-Y	Near NW coast of Kef. isl.	27/02/87	5.7	ST1303
352-Y	Biga	05/07/83	6.1	ST131	1881-X	South Aegean	23/05/94	6.1	ST1310
359-X	Umbria	29/04/84	5.6	ST136	1887-X	Griva	21/12/90	6.1	ST1318
360-X	Umbria	29/04/84	5.6	ST41	1891-Y	Kranidia	25/10/84	5.5	ST1320
362-X	Umbria	29/04/84	5.6	ST137	1908-X	Filippias	16/06/90	5.5	ST126
368-Y	Lazio Abruzzo	07/05/84	5.9	ST143	1959-X	Kyllini	16/10/88	5.9	ST214
369-X	Lazio Abruzzo	07/05/84	5.9	ST109	1984-X	Kefallinia island	23/01/92	5.6	ST1353
373-X	Lazio Abruzzo	07/05/84	5.9	ST147	1996-X	Anchialos	30/04/85	5.6	ST1355
374-Y	Lazio Abruzzo	07/05/84	5.9	ST148	4477-X	Duzce 3 (aftershock)	23/08/00	5.5	ST553
375-Y	Lazio Abruzzo	07/05/84	5.9	ST149	4557-X	Bovec	12/04/98	5.6	ST750
379-X	Lazio Abruzzo (aftershock)	11/05/84	5.5	ST1034	4678-X	South Iceland	17/06/00	6.5	ST2557

Table 9 (continued)

Record	Earthquake	Date	M	Station	Record	Earthquake	Date	M	Station
381-X	Lazio Abruzzo (aftershock)	11/05/84	5.5	ST141	4679-Y	South Iceland	17/06/00	6.5	ST2557
382-X	Lazio Abruzzo (aftershock)	11/05/84	5.5	ST140	5270-X	Mt. Vatnafjoll	25/05/87	6.0	ST2486
383-X	Lazio Abruzzo (aftershock)	11/05/84	5.5	ST153	5271-X	Mt. Vatnafjoll	25/05/87	6.0	ST2483
385-X	Lazio Abruzzo (aftershock)	11/05/84	5.5	ST155	5272-X	Mt. Vatnafjoll	25/05/87	6.0	ST2487
410-X	Golbasi	05/05/86	6.0	ST161	5273-X	Mt. Vatnafjoll	25/05/87	6.0	ST2488
412-Y	Golbasi	06/06/86	5.8	ST161	5798-Y	Gulf of Akaba (aftershock)	23/11/95	5.7	ST2989
435-X	Kyllini	16/10/88	5.9	ST159	6100-X	Kozani	13/05/95	6.5	ST1315
439-Y	Spitak	07/12/88	6.7	ST173	6138-X	Aigion	15/06/95	6.5	ST1330
467-X	Chenoua	29/10/89	5.9	ST181	6144-X	Aigion	15/06/95	6.5	ST1332
474-X	Filippias	16/06/90	5.5	ST123	6145-X	Aigion (aftershock)	15/06/95	5.6	ST1332
502-Y	Racha (aftershock)	03/05/91	5.6	ST200	6262-X	South Iceland	17/06/00	6.5	ST2496
531-X	Racha (aftershock)	15/06/91	6.0	ST201	6265-X	South Iceland	17/06/00	6.5	ST2494
532-Y	Racha (aftershock)	15/06/91	6.0	ST202	6267-Y	South Iceland	17/06/00	6.5	ST2565
548-X	Izmir	06/11/92	6.0	ST43	6269-X	South Iceland	17/06/00	6.5	ST2497
549-Y	Izmir	06/11/92	6.0	ST162	6270-Y	South Iceland	17/06/00	6.5	ST2556
555-X	Kallithea	18/03/93	5.8	ST10	6272-X	South Iceland	17/06/00	6.5	ST2568
572-X	Patras	14/07/93	5.6	ST178	6278-X	South Iceland	17/06/00	6.5	ST2552
595-X	Umbria Marche	26/09/97	5.7	ST83	6327-X	South Iceland (aftershock)	21/06/00	6.4	ST2552
598-X	Umbria Marche	26/09/97	6.0	ST222	6329-Y	South Iceland (aftershock)	21/06/00	6.4	ST2485
601-X	Umbria Marche	26/09/97	5.7	ST224	6331-X	South Iceland (aftershock)	21/06/00	6.4	ST2486
602-X	Umbria Marche	26/09/97	6.0	ST224	6333-X	South Iceland (aftershock)	21/06/00	6.4	ST2487
603-Y	Umbria Marche	26/09/97	5.7	ST225	6336-Y	South Iceland (aftershock)	21/06/00	6.4	ST2563
604-X	Umbria Marche	26/09/97	6.0	ST225	6337-X	South Iceland (aftershock)	21/06/00	6.4	ST2494
605-X	Umbria Marche	26/09/97	5.7	ST84	6341-X	South Iceland (aftershock)	21/06/00	6.4	ST2497
607-Y	Umbria Marche	26/09/97	6.0	ST226	6342-X	South Iceland (aftershock)	21/06/00	6.4	ST2556
620-X	Umbria Marche (aftershock)	06/10/97	5.5	ST83	6422-X	Izmit (aftershock)	13/09/99	5.8	ST3135

Table 9 (continued)

Record	Earthquake	Date	M	Station	Record	Earthquake	Date	M	Station
621-X	Umbria Marche (aftershock)	06/10/97	5.5	ST136	6445-Y	Izmit (aftershock)	11/11/99	5.6	ST3133
626-X	Umbria Marche (aftershock)	06/10/97	5.5	ST222	6446-X	Izmit (aftershock)	11/11/99	5.6	ST3139
627-Y	Umbria Marche (aftershock)	06/10/97	5.5	ST86	6496-X	Duzce 1	12/11/99	7.2	ST3135
628-X	Umbria Marche (aftershock)	06/10/97	5.5	ST226	6499-X	Duzce 1	12/11/99	7.2	ST3140
630-Y	Umbria Marche (aftershock)	06/10/97	5.5	ST228	6606-Y	Izmit (aftershock)	11/11/99	5.6	ST2571
633-Y	Umbria Marche (aftershock)	14/10/97	5.6	ST227	6761-Y	Vrancea	30/08/86	7.2	ST40
637-Y	Umbria Marche (aftershock)	14/10/97	5.6	ST232	6960-X	Izmit (aftershock)	13/09/99	5.8	ST3266
638-X	Umbria Marche (aftershock)	14/10/97	5.6	ST233	6962-X	Izmit (aftershock)	13/09/99	5.8	ST3271
642-X	Umbria Marche (aftershock)	14/10/97	5.6	ST225	6963-X	Izmit (aftershock)	13/09/99	5.8	ST3268
643-X	Umbria Marche (aftershock)	14/10/97	5.6	ST224	6964-X	Izmit (aftershock)	13/09/99	5.8	ST3269
644-Y	Umbria Marche (aftershock)	14/10/97	5.6	ST223	6975-Y	Izmit (aftershock)	13/09/99	5.8	ST3272
645-Y	Umbria Marche (aftershock)	14/10/97	5.6	ST83	6978-Y	Izmit (aftershock)	13/09/99	5.8	ST3273
646-X	Umbria Marche (aftershock)	14/10/97	5.6	ST234	7010-X	Izmit (aftershock)	11/11/99	5.6	ST772
648-X	Umbria Marche (aftershock)	14/10/97	5.6	ST221	7067-X	Altinsac	15/11/00	5.5	ST608
650-X	Umbria Marche (aftershock)	14/10/97	5.6	ST235	7155-Y	Firuzabad	20/06/94	5.9	ST3290
652-X	Umbria Marche (aftershock)	14/10/97	5.6	ST236	7158-X	Firuzabad	20/06/94	5.9	ST3293
759-X	Umbria Marche	26/09/97	5.7	ST265	7161-X	Firuzabad	20/06/94	5.9	ST3296
760-X	Umbria Marche	26/09/97	6.0	ST265	7257-X	Masjed-E-Soleyman	25/09/02	5.6	ST3373

References

Adalier K, Aydingun O (2001) Structural engineering aspects of the June 27, 1998 Adana-Ceyhan (Turkey) earthquake. Eng Struct 23:343–355

Akkar S, Boore DM, Gülkan P (2005a) An evaluation of the strong ground motion recorded during the May 1, 2003 Bingöl Turkey, Earthquake. J Earthq Eng 9(2):173–197

Akkar S, Yazgan U, Gulkan P (2005b) Drift estimates in frame buildings subjected to near fault ground motions. J Struct Eng 131(7):1014–1024

Akkar S, Sucuoglu H, Yakut A (2005c) Displacement based fragility functions for low- and mid-rise ordinary concrete buildings. Earthq Spectra 21(4):901–927

Ambraseys NN, Douglas J, Rinaldis D, Berge-Thierry C, Suhadolc P, Costa G, Sigbjornsson R, Smit P (2004a) Dissemination of European strong-motion data, vol 2. CD-ROM Collection, Engineering and Physical Sciences Research Council, Swindon

Ambraseys NN, Smit P, Douglas J, Margaris B, Sigbjornsson R, Olafsson S, Suhadolc P, Costa G (2004b) Internet site for European strong-motion data. Bollettino di Geofisica Teorica ed Applicata 45(3):113–129

Ancheta TD, Darragh RB, Stewart JP, Seyhan E, Silva WJ, Chiou BSJ, Wooddell KE, Graves RB, Kottke AR, Boore DM, Kishida T, Donahue JL (2014) NGA-West2 database. Earthq Spectra 30(3):989–1005

Araújo M, Macedo L, Marques M, Castro JM (2016) Code-based record selection methods for seismic performance assessment of buildings. Earthq Eng Struct Dyn 45:129–148

Arslan MH (2010) An evaluation of effective design parameters on earthquake performance of RC buildings using neural networks. Eng Struct 32:1888–1898

ASCE 07–05 (2006) Minimum design loads for buildings and other structures. American Society of Civil Engineers, Reston

ASCE 07–10 (2010) Minimum Design Loads for Buildings and other structures. American Society of Civil Engineers, Reston

Askan A, Yucemen MS (2010) Probabilistic methods for the estimation of potential seismic damage: application to reinforced concrete buildings in Turkey. Struct Saf 32(4):262–271

ATC-40 (1996) Seismic evaluation and retrofit of concrete buildings, vol 1–2. Applied Technology Council, California

Bal IE, Crowley H, Pinho R, Gülay FG (2008) Detailed assessment of structural characteristics of Turkish RC building stock for loss assessment models. Soil Dyn Earthq Eng 28:914–932

Bazzurro P, Luco N (2005) Accounting for uncertainty and correlation in earthquake loss estimation. In: *Proceedings of the 9th international conference on structural safety and reliability (ICOSSAR)*, Rome

Bommer JJ, Acevedo AB (2004) The use of real earthquake accelerograms as input to dynamic analysis. J Earthq Eng 8(1):43–91

Cantagallo C, Camata G, Spacone E (2014) Seismic demand sensitivity of reinforced concrete structures to ground motion selection and modification Methods. Earthq Spectra 30(4):1449–1465

Celep Z, Erken A, Taskin B, Ilki A (2011) Failures of masonry and concrete buildings during the March 8, 2010 Kovancılar and Palu (Elazığ) earthquakes in Turkey. Eng Fail Anal 18(3):868–889

D'Ambrisi A, Mezzi M (2005) A probabilistic approach for estimating the seismic response of EP SDOF systems. Earthq Eng Struct Dyn 34:1737–1753

Ersoy U, Ozcebe G (2001) Reinforced concrete. Evrim, Istanbul **(in Turkish)**

Eurocode-8 (2004) Design provisions for earthquake resistance of structures, Part 1: General rules, seismic actions and rules for buildings. European Committee for Standardization, Brussels

FEMA-356 (2000) Prestandard and commentary for seismic rehabilitation of buildings. Federal Emergency Management Agency, Washington DC

FEMA-368 (2001) NEHRP recommended provisions for seismic regulations for new buildings and other structures. Federal Emergency Management Agency, Washington (DC)

FEMA-440 (2005) Improvement of nonlinear static seismic analysis procedures. Federal Emergency Management Agency, Washington DC

Gamst G, Meyers LS, Guarino AJ (2008) Analysis of variance designs—a conceptual and computational approach with SPSS and SAS. Cambridge University Press, Cambridge

García RJ, Miranda E (2006) Residual displacement ratios for assessment of existing structures. Earthq Eng Struct Dyn 35:315–336

García RJ, Miranda E (2007) Probabilistic estimation of maximum inelastic displacement demands for performance-based design. Earthq Eng Struct Dyn 9:1235–1254

García RJ, Miranda E (2010) Probabilistic estimation of residual drift demands for seismic assessment of multi-story framed buildings. Eng Struct 32:11–20

GB (2010) Code for seismic design of buildings. China Architecture and Building Press, Beijing
Geem ZW, Kim JH, Loganathan GV (2001) A new heuristic optimization algorithm: harmony search. Simulation 76(2):60–68
Ghaffarzadeh H, Talebian N, Kohandel R (2013) Seismic demand evaluation of medium ductility RC moment frames using nonlinear procedures. Earthq Eng Eng Vib 12:399–409
Han SW, Ha SJ, Seok SW (2014) Efficient and accurate procedure for selecting ground motions matching target response spectrum. Nonlinear Dyn 78(2):889–905
Hancock J, Bommer JJ, Stafford PJ (2008) Numbers of scaled and matched accelerograms required for inelastic dynamic analyses. Earthq Eng Struct Dyn 37:1585–1607
Hatzigeorgiou GD, Beskos DE (2009) Inelastic displacement ratios for SDOF structures subjected to repeated earthquakes. Eng Struct 31:2744–2755
Hatzigeorgiou GD, Liolios AA (2010) Nonlinear behaviour of RC frames under repeated strong ground motions. Soil Dyn Earthq Eng 30:1010–1025
Hou H, Qu B (2015) Duration effect of spectrally matched ground motions on seismic demands of elastic perfectly plastic SDOFS. Eng Struct 90:48–60
Iervolino I, Maddaloni G, Cosenza E (2008) Eurocode 8 compliant real record sets for seismic analysis of structures. J Earthq Eng 12:54–90
Iervolino I, Galasso C, Cosenza E (2010a) REXEL: computer aided record selection for code-based seismic structural analysis. Bull Earthq Eng 8:339–362
Iervolino I, De Luca F, Cosenza E (2010b) Spectral shape-based assessment of SDOF nonlinear response to real, adjusted and artificial accelerograms. Eng Struct 32(9):2276–2792
Ilki A, Celep Z (2012) Earthquakes, existing buildings and seismic design codes in Turkey. Arab J Sci Eng 37:365–380
Inel M, Ozmen HB, Bilgin H (2008) Re-evaluation of building damage during recent earthquakes in Turkey. Eng Struct 30:412–427
Katsanos EI, Sextos AG (2013) ISSARS: an integrated software environment for structure-specific earthquake ground motion selection. Adv Eng Softw 58:70–85
Katsanos IE, Sextos GA, Manolis DG (2010) Selection of earthquake ground motion records: a state- of-the- art- review from a structural engineering perspective. Soil Dyn Earthq Eng 30:157–169
Kayhan AH (2016) Scaled and unscaled ground motion sets for uni-directional and bi-directional dynamic analysis. Earthq Struct 10(3):563–588
Kayhan AH, Demir A (2016) Statistical evaluation of drift demands of rc frames using code-compatible real ground motion record sets. Struct Eng Mech 60(6):953–977
Kayhan AH, Korkmaz KA, Irfanoglu A (2011) Selecting and scaling real ground motion records using harmony search algorithm. Soil Dyn Earthq Eng 31:941–953
Korkmaz S (2015) Observations on the Van earthquake and structural failures. J Perform Constr Facil 29(1):04014033
Lin L (2008) Development of improved intensity measures for probabilistic seismic demand analysis. Ph.D. thesis, Department of Civil Engineering, University of Ottawa, Canada
Lin Y, Miranda E (2009) Estimation of maximum roof displacement demands in regular multistory buildings. J Eng Mech 136:1–11
Luzi L, Puglia R, Russo E, ORFEUS WG5 (2016) Engineering strong motion database, version 1.0. Istituto Nazionale di Geofisica e Vulcanologia, Observatories and Research Facilities for European Seismology. https://doi.org/10.13127/esm
Macedo L, Castro JM (2017) SelEQ: an advanced ground motion record selection and scaling framework. Adv Eng Softw. https://doi.org/10.1016/j.advengsoft.2017.05.005
Mander JB (1984) Seismic design of bridge piers, research report 84-2. Department of Civil Engineering, University of Canterbury, Christchurch
Medina AR, Krawinkler H (2005) Evaluation of drift demands for the seismic performance assessment of frames. J Struct Eng 7:1003–1013
Mitseas IP, Kougioumtzoglou IA, Beer M (2016) An approximate stochastic dynamics approach for nonlinear structural system performance-based multi-objective optimum design. Struct Saf 60:67–76
Naeim F, Alimoradi A, Pezeshk S (2004) Selection and scaling of ground motion time histories for structural design using genetic algorithm. Earthq Spectra 20(2):413–426
Palanci M, Kalkan A, Senel SM, Yilmaz Y (2014) Investigation of effect of different modeling techniques on existing buildings performance. In: *11th international congress on advances in civil engineering*, Oct 21–25, Istanbul
Palanci M, Kalkan A, Senel SM (2016) Investigation of shear effects on the capacity and demand estimation of RC buildings. Struct Eng Mech 60(6):1021–1038

Priestley MJN, Calvi GM, Kowalsky MJ (2007) Displacement-based seismic design of structures. IUSS Press, Pavia

Reyes JC, Kalkan E (2012) How many records should be used in an ASCE/SEI-7 ground motiom scaling procedure. Earthq Spectra 28(3):1223–1242

SAP2000 (2009) Integrated solution for structural analysis and design. Computers and Structures, Berkeley

Scott BD, Park R, Priestley MJN (1982) Stress–strain behavior of concrete confined by overlapping hoops at low and high strain rates. ACI Struct J 76(1):13–27

SEAOC Vision Committee 2000 (1995) Performance-based seismic engineering. Report prepared by Structural Engineers Association of California, Sacramento

Sextos AG, Katsanos EI, Manolis GD (2011) EC8-based earthquake record selection procedure evaluation: validation study based on observed damage of an irregular R/C building. Soil Dyn Earthq Eng 31:583–597

Sezen H, Elwood KJ, Whittaker AS, Mosalam KM, Wallace JW, Stanton JF (2000) Structural engineering reconnaissance of the August 17, 1999 earthquake: Kocaeli (Izmit), Turkey. Report 2000-09, Pasific Earthquake Engineering Research Center, University of California, Berkeley

Shome N, Cornell AC, Bazzurro P, Carballo JE (1998) Earthquakes, records and nonlinear responses. Earthq Spectra 14:469–500

Taskin B, Sezen A, Tugsal UM, Erken A (2013) The aftermath of 2011 Van earthquakes: evaluation of strong motion, geotechnical and structural issues. Bull Earthq Eng 11(1):285–312

TEC-1975 (1975) Specification for structures to be built in disaster areas, Turkish earthquake code. Ministry of Public Works and Settlement, Ankara **(in Turkish)**

TEC-1997 (1997) Specification for structures to be built in disaster areas. Ministry of Public Works and Settlement, Ankara, Turkish Earthquake Code

TEC-2007 (2007) Specification for structures to be built in disaster areas, Turkish earthquake code. Ministry of Public Works and Settlement, Ankara

TS-500 (2000) Requirements for design and construction of reinforced concrete structures. Turkish Standards Institute, Ankara

Watson-Lamprey J, Abrahamson N (2006) Selection of ground motion time series and limits on scaling. Soil Dyn Earthq Eng 26:477–482

Yamin LE, Hurtado A, Rincon R, Dorado JF, Reyes JC (2017) Probabilistic seismic vulnerability assessment of buildings in terms of economic losses. Eng Struct 138:308–323

Yon B, Sayin E, Koksal TS (2013) Seismic response of buildings during the May 19, 2011 Simav, Turkey earthquake. Earthq Struct 5(3):343–357